Submitted to ADVANCED FUNCTIONAL MATERIALS

DOI: 10.1002/adfm.((please insert DOI)

Towards a Universal Method for the Stable and Clean Functionalization of Inert Perfluoropolymer Nanoparticles: Exploiting Photopolymerizable Amphiphilic Diacetylenes

By *Carlo Morasso*, *Miriam Colombo*, *Silvia Ronchi*, *Laura Polito*, *Diego Monti*, *Marco Buscaglia*, *Tommaso Bellini* and *Davide Prosperi**

[*] Dr. D. Prosperi, M. Colombo
Dipartimento di Biotecnologie e Bioscienze
Università degli Studi di Milano-Bicocca
Piazza della Scienza 2, 20126 Milan (Italy)
E-mail: davide.prosperi@unimib.it
Dr. C. Morasso,[+] Dr. D. Prosperi, Dr. D. Monti, Dr. S. Ronchi, Dr. L. Polito
Istituto di Scienze e Tecnologie Molecolari, CNR
via Fantoli 16/15, 20138 Milan (Italy)
Dr. M. Buscaglia, Prof. Dr. T. Bellini
Dipartimento di Chimica, Biochimica e Biotecnologie per la Medicina
Università degli Studi di Milano
Via F.lli Cervi 93, 20090 Segrate (Italy)
[+] Current address: London Centre for Nanotechnology, University College London, 17-19 Gordon Street, London WCIH OAL (UK)

Keywords: colloids; perfluoropolymer; functional coating; surface modification; photochemistry

Highly fluorinated materials are being widely investigated due to a number of peculiar properties, potentially useful for various applications, including use as lubricants, antiadhesive films and substitutes of biological fluids for biomedical utilization. However, at present such potential is still poorly exploited. One of the major drawbacks, which hampers the rapid development of nanoscale fluoro-hybrid devices, resides in the remarkable inertness of perfluoropolymeric materials lacking reactive functionalities, as they do not offer any functional group that can be employed to covalently anchor organic molecules on their surface. In this paper, we report a convenient method for the stable biofunctionalization of strongly unreactive perfluoropolymer nanoparticles (PnPs). PnPs are easily coated with newly

synthesized asymmetrical diacetylenic monomer compounds (ADMs), thanks to PnP high propensity to interact with hydrophobic moieties. Once monomerically adsorbed on PnPs, such suitably designed ADMs enable the formation of a robust polymeric shell around the perfluoroelastomer core *via* a clean UV-promoted localized photopolymerization. The potential of this method for the biofunctionalization of PnPs is demonstrated with representative proteins and carbohydrates. Among them, the extension to avidin-biotin technology may broaden the scope and applicability of this strategy potentially to a large number of molecules of biomedical interest.

1. Introduction

Highly fluorinated molecular, macromolecular, or supramolecular materials are being intensely investigated and used, due to a number of peculiar properties, which are potentially useful for biomedical applications, including exquisite chemical and biological inertness, biocompatibility, high contact angle with water, capability to translate into low friction materials, intrinsically low refractive index, absence of protons and such a concentration of ^{19}F spin-active nuclei that provide a valuable probe for magnetic resonance imaging (MRI).[1] Perfluoroelastomer and perfluoropolyether compounds do not spring from Nature, yet they can offer useful building blocks for the design of novel functional biopolymers and clever solutions to physiologically vital issues, which have attracted much attention from several research groups.[2] Recently, by exploiting the low refractive index of one of these materials, we developed a novel biosensor based on the measurement of the intensity of the light scattered by index-matched perfluoroelastomer colloids.[3-6]

Light scattering provides a versatile and non-invasive method to study structures and phenomena taking place at the mesoscale level, such as aggregative events, thus becoming a crucial characterization tool in colloidal science. Nevertheless, light scattering is not a conventional technique to study molecular association because the binding of isolated ligands

and receptors in dilute solutions produces negligible increment of the scattered light intensity,[7] while micrometer scale particles hosting multiple receptors, for instance entire cells, intrinsically scatter too much light compared to the specific contributions due to molecular interactions. This limitation can be overcome by supporting the receptors on nanoscale perfluorinated latex spheres (80 nm diameter), whose refractive index closely matches the one of water ("phantom" nanoparticles, PnPs). When molecular interactions take place at the surface of PnPs, the coherent enhancement of the scattering signal, originated from the docking of ligand and receptor molecules, exceeds the background scattering from the particles. The amount of (bio)organic matter, together with the affinity of the interactions occurring at the PnP surface, can be precisely deduced by accurate measurement of the scattered intensity.[3,4] The resulting simple method, called "dispersed phantom scatterer" (DPS), is sensitive and particularly suitable to investigate binding phenomena at the solid-liquid interface.

Unfortunately, in many instances, perfluoropolymeric materials, including PnPs, cannot be easily functionalized, as they do not offer any reactive group that can be used to covalently anchor a receptor to the particles. The hard difficulties encountered by those who attempt to chemically modify highly fluorinated surfaces represent a major limitation to the rapid development of nanoscale hybrid materials based on perfluoropolymer systems beyond the current achievements. To avoid the obstacle, two main approaches have been used traditionally: the first is to generate a self-assembled surfactant monolayer, exploiting the high propensity of perfluoropolymer water suspensions to interact with hydrophobic moieties by entropic stabilization. Second, it has been observed that hydrophobic model surfaces, such as PTFE, induce protein reversible adsorption.[8-10] However, direct adsorption of proteins is generally useless, as this process is often associated with protein denaturation,[11] and no control is possible at present to limit undesired detachment from the fluorinated surface. For

these reasons, novel methods providing the immobilization of intermediate pro-functional anchors suitable for bioconjugation are highly desired.[12]

Amphiphilic polymers have been used so far for coating hydrophobic nanoparticles;[13-16] they usually consist of hydrophobic side chains for the linkage to the nanoparticle surface and a hydrophilic backbone that provides water solubility through polar groups and additionally acts as an anchor for the attachment of biological molecules. As the stability of the amphiphilic coating depends exclusively on the number and distribution of hydrophobic interactions, the procedure can be reversible to some extent, giving rise to unstable dispersions. With the aim of improving the stability of these colloidal solutions, we have developed novel diacetylenic amphiphilic molecules that, once adsorbed on the surface of PnPs, are able to cross-polymerize by UV irradiation with an excitation wavelength in the range 240-280 nm. Ordered diacetylene layers, indeed, are known to undergo photopolymerization *via* 1,4-addition to form an ene-yne alternating polymer chain after UV irradiation, commonly termed as polydiacetylene (PDA).[17-19] In this paper, we report a reliable method for the successful functionalization of perfluoroelastomer nanoparticles *via* newly synthesized asymmetrical diacetylenic monomer compounds (ADMs, Fig. 1), and we present the results of our studies on ADM adsorption on PnPs and their UV-promoted polymerization. Suitably designed diacetylenic compounds, obtained as water-soluble monomers, enabled the formation of a robust polymeric shell around the PnP core, displaying the functional groups on the outer surface of the nanospheres. ADMs were quickly adsorbed on PnP surface in aqueous solution: due to the high solubility of these surfactant molecules, we were allowed to consider all the added material to be actually adsorbed, enabling us to calculate the amount of available receptors displayed on PnPs. In this way, the particles acted as a template, inducing self-assembling of amphiphilic diynes. The strategy reported here resulted highly advantageous because it made possible to fully characterize the ADMs before

the actual coating of the particles, and the subsequent UV-mediated cross-linking was a "green" and safe procedure, as it avoided the use of toxic coupling agents (such as glutaraldehyde, carbodiimides or epichlorohydrin) that are commonly employed to stabilize particle coatings.[20-22]

2. Results and Discussion

2.1 Chemistry

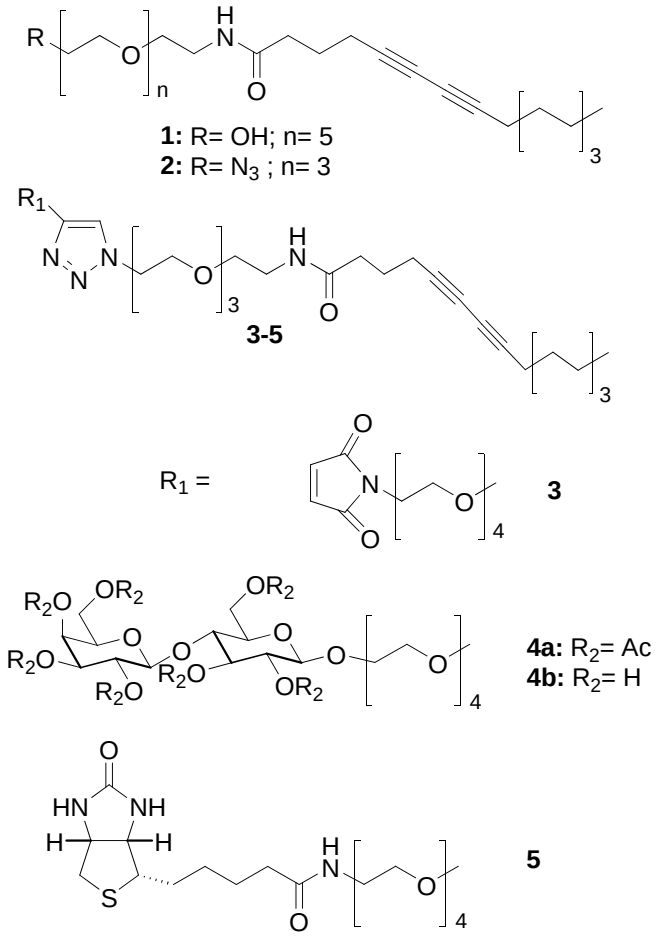

Figure 1. Novel ADMs useful for PnP coating.

First, a bio-inert oligo(ethylene glycol)-based amphiphile (**1**), depicted in Figure 1, was synthesized as non-interacting surfactant to limit any accidental adhesion. Then, starting from the diacetylenic scaffold (**2**) and exploiting the 1,3-dipolar Huisgen "click" cycloaddition,[23-24] we obtained a small library of ADMs (**3-5**). Each one of them was designed either to promote the formation of a covalent bond or to specifically interact with the

appropriate biomolecular counterpart in order to afford a tunable and stable connection or recognition, respectively. The maleimido function (**3**) is largely used to react with cysteine residues often available in proteins via a Michael addition on the electron-poor double bond;[25] lactose (**4**) is able to specifically bind lectins and to interact head-to-head with other lactose moieties *via* a Ca^{2+}-mediated recognition;[26,27] biotin (**5**) binds avidin with the strongest known biological interaction.[28,29] Compound **1** was obtained from the condensation of commercially available 5,7-hexadecadiynoic acid with monoamino-modified hexaethylene glycol obtained *via* statistical formation of the corresponding azido precursor **7a**. The reaction was triggered by activation of 5,7-hexadecadiynoic acid with *N*-hydroxysuccinimide, affording the polymerizable ADM **1** in a moderate yield (Scheme 1).

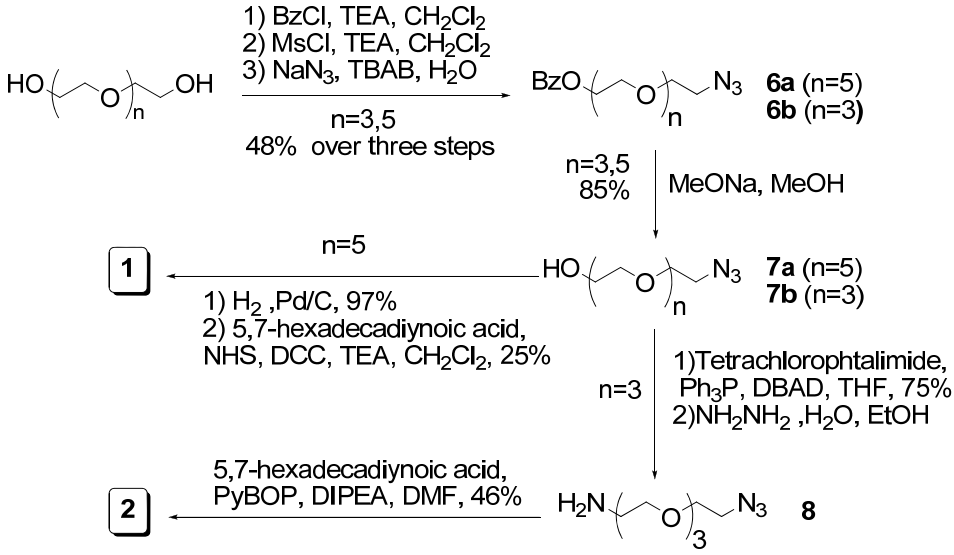

Scheme 1. Stepwise synthesis of ADMs **1** and **2**. (TBAB = tetrabutylammonium bromide; NHS = *N*-hydroxysuccinimide; DCC = *N*,*N*′-dicyclohexylcarbodiimide; DIPEA = diisopropylethylamine)

Similar to the synthesis of **1**, azido diacetylenic scaffold **2** was prepared starting from tetraethylene glycol. Compound **7b** was then converted into the amino derivative **8** by a Mitsunobu reaction. Because of the presence of an azido group on the molecule, it was necessary to pre-activate triphenylphosphine by di-*t*-butyl-azodicarboxylate (DBAD) to prevent the formation of an iminophosphorane, which is an undesired Staudinger adduct of

the reaction. The final amine **8** was then obtained via the Ing-Manske procedure,[30] involving a reaction with hydrazine in refluxing ethanol. Compound **2** was then obtained using benzotriazol-1-yl-oxytripyrrolidinophosphonium hexafluorophosphate (PyBOP) as coupling reagent. The synthesis of the propargyl derivatives is depicted in Scheme 2.

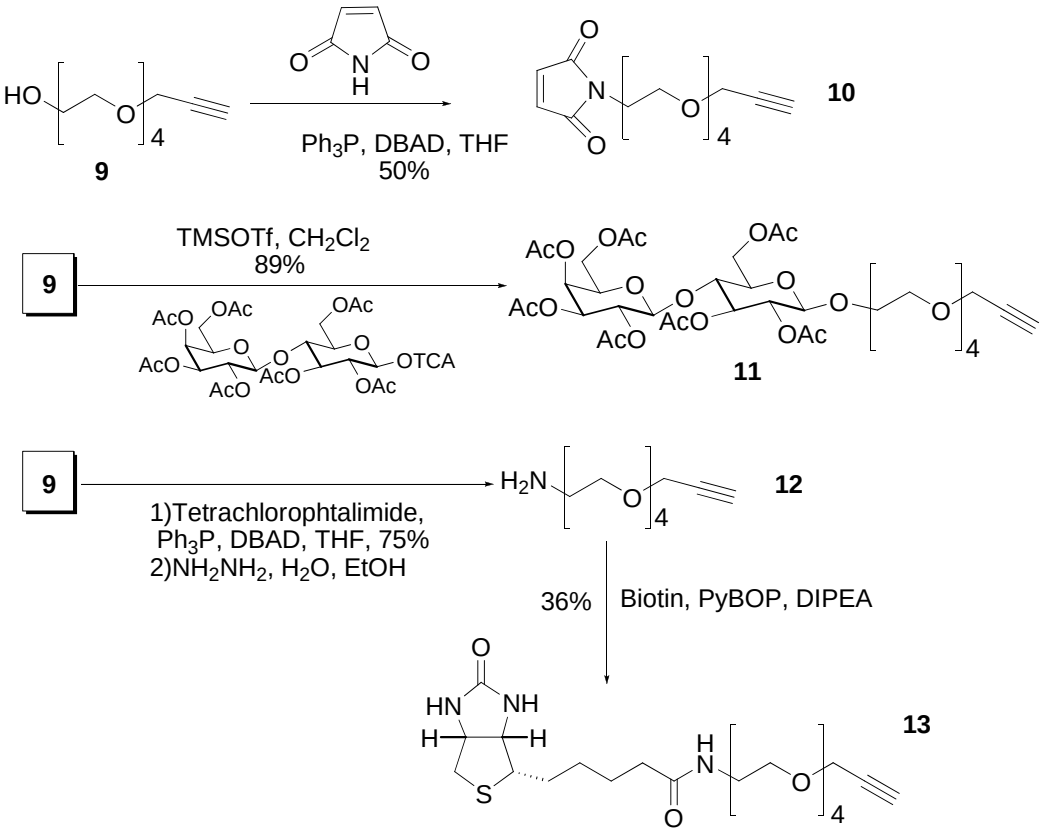

Scheme 2. Preparation of the pro-functional alkyne-bearing units.

The starting building block **9**[31] was converted into **10** *via* Mitsunobu reaction, optimized using polymer-bound Ph_3P to facilitate the removal of Ph_3PO, which is an undesired byproduct of the reaction. The peracetylated lactosyl derivative **11** was instead the result of a glycosylation, following the popular Schmidt procedure.[32] For the preparation of the modified biotin **13**, it was necessary to change the free hydroxyl group of **9** into the corresponding amine **12**. The "click" reactions were performed under different conditions, as detailed in the Supporting Information (SI). Unfortunately, when an alcohol was present in the system as co-solvent, some problems of solubility occurred. In order to overcome these

problems, a biphasic system consisting of a mixture of water and dichloromethane was employed, resulting in better yields.

2.2 Studies of PnP Coating and Photopolymerization

ADM **1** was selected as the polymerizable model monomer to test the PnP coating performance and to optimize the photopolymerization conditions. This product was readily adsorbed onto PnPs, as previously observed for commercial nonionic surfactants.[3]

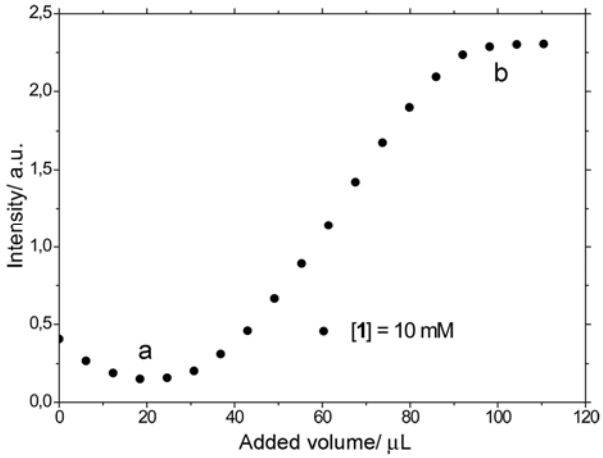

Figure 2. Scattered light intensity of a PnP dispersion as a function of the added amount of surfactant **1**.

Figure 2 shows a typical readout of a PnP coating experiment obtained by adding purified ADM **1** to the nanoparticle suspension. The changes in the scattered intensity were registered following the PnP coverage by consecutive addition of controlled amounts of adsorbing material. Initially, as the starting refractive index of PnP is slightly lower than the one of water, the intensity decreased down to a minimum corresponding to the perfect index-match (a).[3] Beyond that value, the slope of the curve increased, following a Langmuir isotherm-like behavior, in dependence of the mass of matter adsorbing on the surface of the scattering colloids up to a plateau (b), which corresponds to the PnP full coverage. Further additions did not induce any changes in the overall scattering intensity, as the hydrophobic surface could not accommodate further surfactant molecules. Notably, the resulting curve (Fig. S1 in SI) could be fitted by a monoexponential function providing us with the parameters

needed for determination of the affinity of the molecular layer for the PnP surface, which exhibited a $k_d = 6.1 \times 10^{-6}$ M. This is the essence of a DPS experiment, which allowed us to accurately determine several useful parameters, including the mass of material adsorbed, and the affinity of the surfactant molecules for the interacting surface. The polymerization of **1** was achieved by exposing the dispersion of **1**-coated PnPs to a 266 nm laser irradiation, which generated an organic polymer shell covering the fluorinated surface. The positive outcome of the photopolymerization was evidenced by the appearance of a light-orange coloring, resulting from the formation of a distorted polyconjugated backbone (Fig. 3).[33,34]

Figure 3. Water dispersion (0.1% v/v) of **1**-coated PnPs before (left) and after (right) photopolymerization promoted by 15 min exposure to 266 nm UV laser light.

The UV-vis spectra of **1**-coated PnPs, recorded at 5 min intervals during UV irradiation, showed a marked increase of ε up to a maximum value, which was reached after 15 min, corresponding to the polymerization completion (Fig. 4A). Notably, the polymer coating exhibited also a fluorescence emission with λ_{ex} = 390 nm and λ_{em} = 495 nm (Fig. S2 in SI).

Next, dynamic light scattering (DLS) provided us with evidence that the polymerized **1**-coated PnPs (**PDA-1**) were monomerically dispersed after 20 min UV exposure, after which larger aggregates began to form (Fig. 4B). By comparing the results of these two experiments, we concluded that the optimal time of exposure to obtain the maximal extent of surface

polymerization while minimizing the formation of interparticle crosslinks, was 15 min. Hence, the following experiments were performed using such time of exposure.

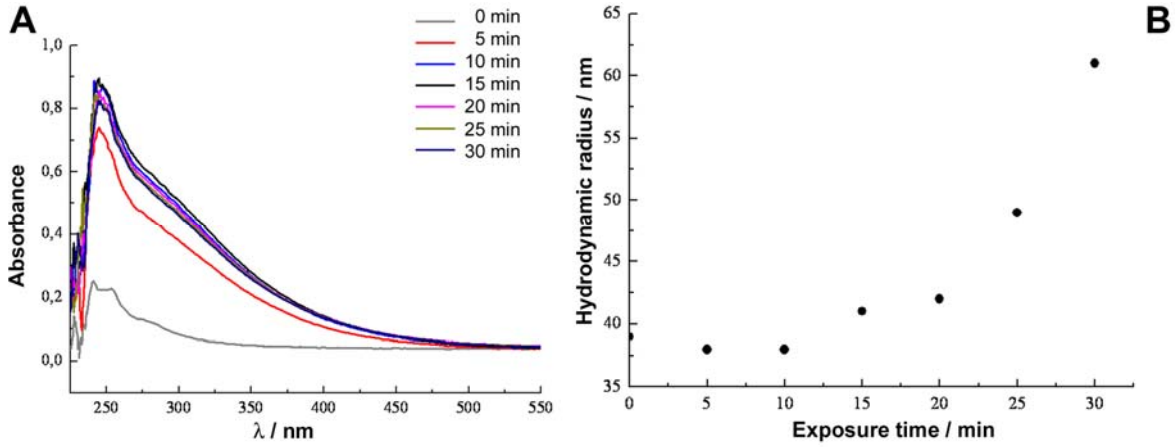

Figure 4. A) Absorbance profiles of adsorbed monomers (grey line) and of the photopolymerizing film (other lines) acquired at 5 min intervals. The maximal intensity was reached after 15 min (black line). B) Hydrodynamic radius of **1**-coated PnPs in dependence of the time of exposure to 80 mW UV irradiation at 266 nm. After 20 min, a considerable increase was detected due to the formation of large agglomerates triggered by interparticle polymerization.

A further control experiment was performed to assess whether the polymerized surfactant was indeed adsorbed onto PnPs rather than free micelles were also present in solution: repeated DLS analyses of a solution of ADM **1** in deionized water invariably showed a mean hydrodynamic radius in the range 1-2 μm, remarkably higher than that observed for **PDA-1** nanoparticles (Fig. S3 in SI).

PDA-1 were stable in water and did not show nonspecific interactions with proteins (*e.g.*, BSA). In fact, after the addition of BSA, no significant increment of scattered light was observed either with monomeric or polymeric forms of the surfactant adsorbed onto PnPs (Fig. 5). Next, we calculated the amount of ADM **1** adsorbed onto the PnPs. Given the number of ligand additions, each one of them being precisely quantified (6×10^{-5} mmol), we determined that about 8.4×10^4 molecules were necessary to completely cover each PnP. Since the average surface area of one PnP is 2.01×10^4 nm^2, ca. 4.1 molecules/nm^2 could be

accommodated on the surface of each PnP, which is consistent with a monolayer-like packaging of polymerized **1**, as schematically represented in Scheme 3. This experiment was repeated several times, invariably obtaining the same number of coating molecules (SD = ± 450 molecules), which allowed us to exclude an alternative unordered molecular distribution, such as the formation of multilayers. The observed little uncertainty (ca. 0.5%) can be explained in terms of the presence of a small fraction of molecules that are not involved in the polymerized film. We argued that these "free" ADMs could be necessary to reduce the molecular strain due to the curvature of the nanoparticle surface. Within this model, we concluded that the photopolymerized monolayer was more probably organized in compacted blocks separated by small "cracks" in correspondence of clusters of ADMs then in a continuous film. A further confirmation for this came out from the experiment reported in Figure 6B, which will be discussed below.

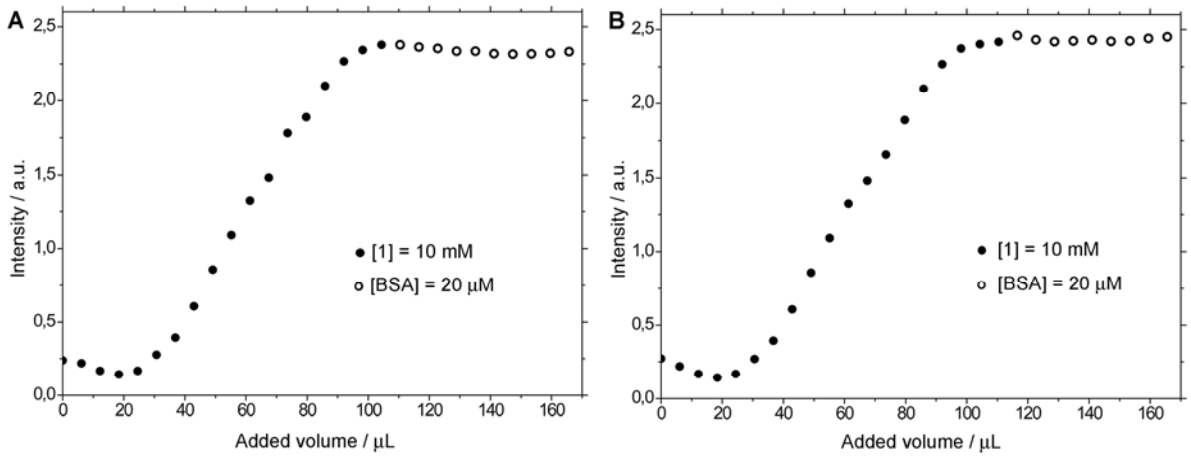

Figure 5. Scattered light intensity of a 0.1% v/v PnP dispersion as a function of the added amount of ADM **1** (full dots) followed by BSA additions (empty dots). BSA was reacted with PnPs coated with **1** before (**A**) and after (**B**) photopolymerization.

The **PDA-1** nanoparticles could be centrifuged and redispersed in water several times to remove the possible traces of unbound **1** and the possible presence of micelles. Finally, dried **PDA-1** nanoparticles were observed at attenuated total reflection (ATR) and Micro-FTIR and the resulting IR scan spectra were compared with the FTIR spectrum of ADM **1** (Fig. S4 in

SI). Besides the expected weak signal of C≡C stretching at 2123 cm^{-1}, we observed a marked left-side broadening in the strong absorption of C=O at 1650 cm^{-1}, which could be explained with the appearance of one supplementary small peak in the range 1660-1670 cm^{-1} attributable to a weak C=C symmetric stretching, accounting for the formation of new quaternary conjugated *ene* functional groups.

2.3 Determination of Coating Stability

In order to check the actual extent of polymerization of **1** onto PnPs, a desorption test was implemented. To this aim we added smaller perfluorinated latex nanospheres to the solution as competitive substrate to induce surfactant sequestration from PnPs. We used the 20 nm radius nanoparticles (PP20) previously characterized in ref.[4] Their size, half of PnPs, ensured that they could provide a large competing surface without contributing significantly to the measured scattering, as discussed below.

The rationale of the desorption experiment is pictured in Figure 6A, where a typical adsorption curve such as that of Figure 2 is plotted as a function of added surfactant (lower x axis). With $I_A(c)$, we indicate the scattered intensity vs. surfactant concentration in the adsorption experiment. In the desorption experiment, PnPs were first fully coated reaching the point labelled (a) in the figure, corresponding to an amount c_a of surfactant added to the dispersion and almost entirely adsorbed on the particles. Then, a concentrated dispersion of PP20 is progressively added, thus increasing the total surface made available to the surfactant to adsorb on. As this happens, surfactant is desorbed from the PnPs, resulting in an overall decreased scattered intensity, as indicated in Figure 6A (top x axis).

Experimental results are reported in Figure 6B as a function of the ratio X = S(PP20)/S(PnP) between the total surface area S of PP20 and PnPs available in the suspension as the PP20 are added in. With $I_D(X)$ we indicate the scattered intensity vs. surfactant concentration in the desorption experiment. Plotted $I_D(X)$ data are already corrected for

dilution effects. The desorption experiment has been performed with non-polymerized surfactants (lower triangles) and with coated PnPs after various durations of UV irradiation, the longest being 20 minutes (full dots). In the same figure we plotted an estimate (dot-dashed line) of the contribution from PP20 to the total scattering. Given the size ratio of the particles, the scattering cross section of each PP20, when fully coated by surfactant, is about 1/16 of that of PnPs. On this basis, the estimate followed by assuming an even partitioning of the surfactant, originally adsorbed on the PnPs, on all the available surface. As visible, the PP20 contribution to the signal was minor. In the following analysis, we have approximated the contribution as a constant (dot-dashed line in Fig. 6A), which has been added to the scattering of PnPs to obtain the continuous line in Figure 6A.

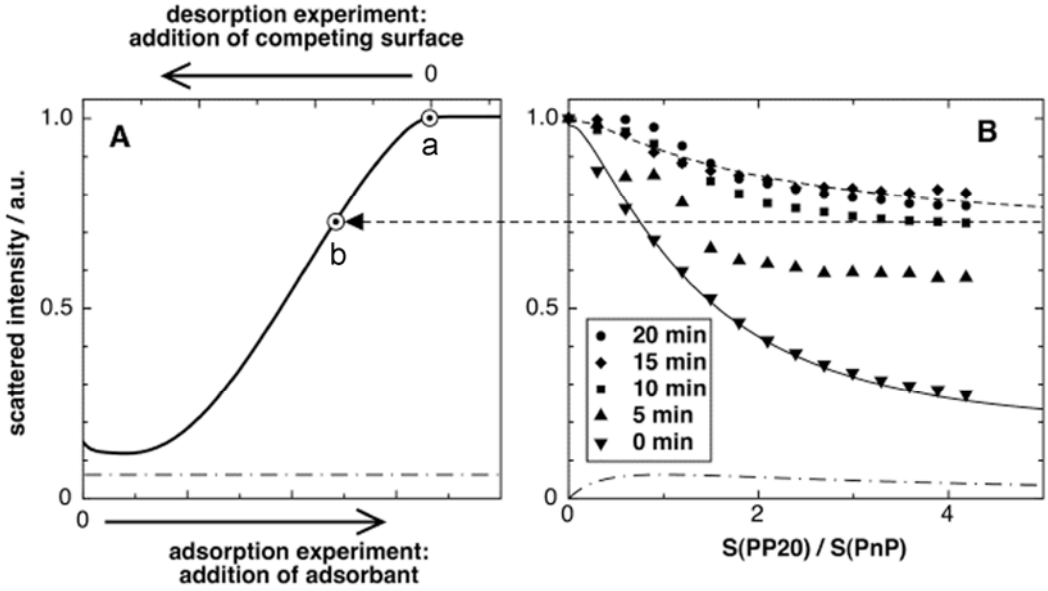

Figure 6. A) Scattered intensity as a function of the added surfactant in the adsorption experiment (lower x axis) and as a function of the added bare surface in the desorption experiment (upper x axis). The curve in figure is obtained by adding the scattered intensity reported in Figure 2 to the background due to the PP20 particles (dot-dashed line). (a) and (b) indicate, respectively, fully coated particles, particles partially uncoated by the surfactant sequestration by the competing surfaces. B) Scattered intensity measured in the desorption experiments as a function of the ratio of the total surface of PP20 and PnPs. Symbols indicate various UV exposure times (see legend). The dot dashed line is an estimate of the contribution of PP20 to the total scattering. The continuous line and the dashed lines are obtained by fitting the data as described in the text.

We have thus fitted the $I_D(X)$ data for non-polymerized surfactant on the basis of $I_A(c)$, previously measured. To do so, we have exploited the identity $I_D(X) = I_A(c_a/(1+kX))$, where $(1+X)^{-1}$ is the ratio of the surface of PnPs to the total colloidal surface. We have also introduced the parameter k to indicate a possible preferential adsorption on one of the two species. $I_D(X)$ measured for non-polymerized surfactant can be well represented with this equation provided that $k \sim 0.7$. This result supports the notion that monomeric surfactant molecules are only weakly tied on PnPs. Upon addition of bare PP20 particles, surfactant molecules rapidly migrated from the coated PnPs to the bare nanoparticles until a new equilibrated distribution was reached.

In contrast, the formation of surfactant chains by photopolymerization increases the effective size of the hydrophobic anchor and thus the interactions with the hydrophobic surfaces. The spontaneous desorption and redistribution of polymerized surfactants requires larger activation energy and becomes much less significant. This is indicated by the $I_D(X)$ data in Figure 6B, where, after 10 minutes of exposure to UV radiation, the decrease of scattered intensity as bare PP20 are added in, is much less significant than in the non-polymerized case.

Data can be interpreted by assuming that the surfactant on the PnPs is partitioned in polymerized groups that do not desorb, and in a small fraction of non-polymerized monomers that evenly distribute on all the available surfaces. Specifically, we have assumed that the surfactant desorbs from PnPs so to reach the position (b) in Figure 6A, while the surfactant providing the scattering $I_A(c_b)$ is stabilized by the polymerization. The position of (b) can be determined by fitting the $I_D(X)$ data for the polymerized surfactants according to this double-population model, where the free parameter is the fraction of non-polymerized surfactant. The resulting curve is shown in Figure 6B for the more intensely UV-irradiated particles (full dots). The asymptote of the fitting curve determines the position (b) on the $I_A(c)$ curve

(dashed construction in Fig. 6B), in turn enabling to quantify the fraction c_b/c_a of polymerized surfactant. Specifically, we obtained that 10 minutes of UV irradiation were enough to crosslink more then 70% of the adsorbed surfactant molecules, while longer exposures did not increase the polymerized fraction.

2.4 Biofunctionalization of PnP Surface

Eventually, we evaluated the capability of perfluoroelastomer colloids, in which reactive functional groups were introduced by our method, to serve as a convenient bioconjugation platform for the facile functionalization with complex biomolecules, such as proteins. Scheme 3 illustrates a representative strategy using human serum albumin (HSA). Consecutive additions of a mixture of ADMs **1** and **3** in a 400:1 ratio were added to the bare PnPs, thus generating a monolayer of insulated **3** intercalated by clustered groups of **1**. This mixed layer was polymerized on the PnP surface following the UV laser-promoted procedure described above. This generated a large number of maleimido groups, which could be easily linked to HSA by Michael addition at the thiol group of its natively unpaired Cys34 residue.[31] The number of anchored proteins was determined by elastic light scattering to be 86 per PnP (Fig. 7A, detailed calculation is reported in SI).

Analogous procedures were successfully repeated with compounds **4b** and **5**, using galectin-3 and streptavidin (SAv), respectively, as recognizing counterparts, testifying to the generality of the method. To a PnP dispersion functionalized with a mixture of **1** and **5** were first added small aliquots of SAv resulting in the rapid formation of interparticle aggregates due to PnP crosslinking events induced by the strong recognition of tetrameric SAv with biotin molecules linked to the surface of different PnPs (Fig. 7B). The same experiment performed in absence of biotin by using **1**-coated PnPs as substrate, resulted in no aggregation, confirming that the above phenomena could not be ascribed to nonspecific interactions (Fig. 7C). Analogously,

galectin-3 exhibited the tendency to form large aggregates triggered by cooperative binding with anchored lactose units (Fig. 7D).

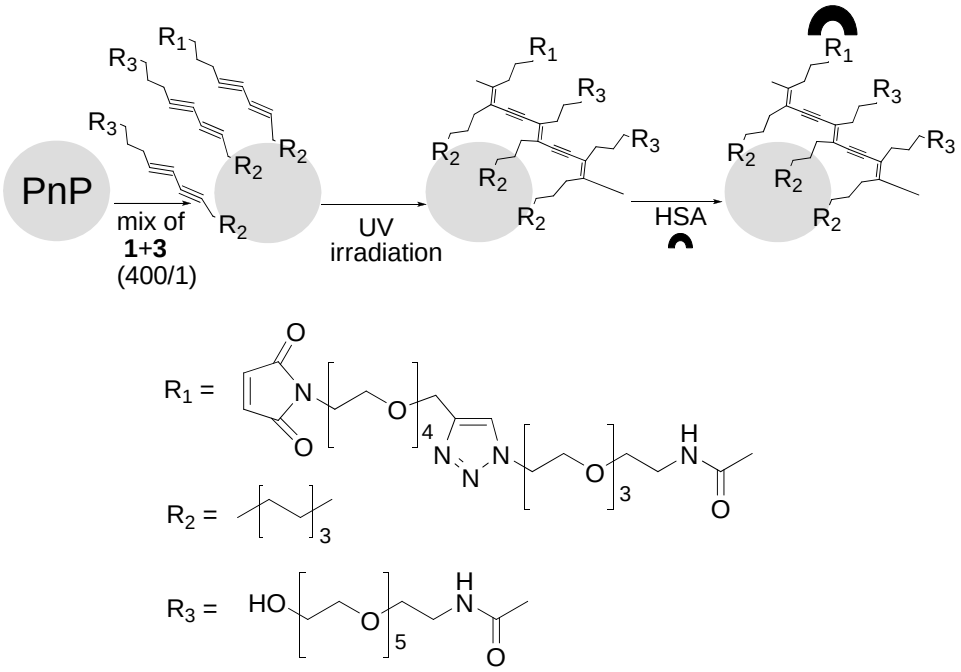

Scheme 3. Schematic strategy for the biofunctionalization of bare PnPs.

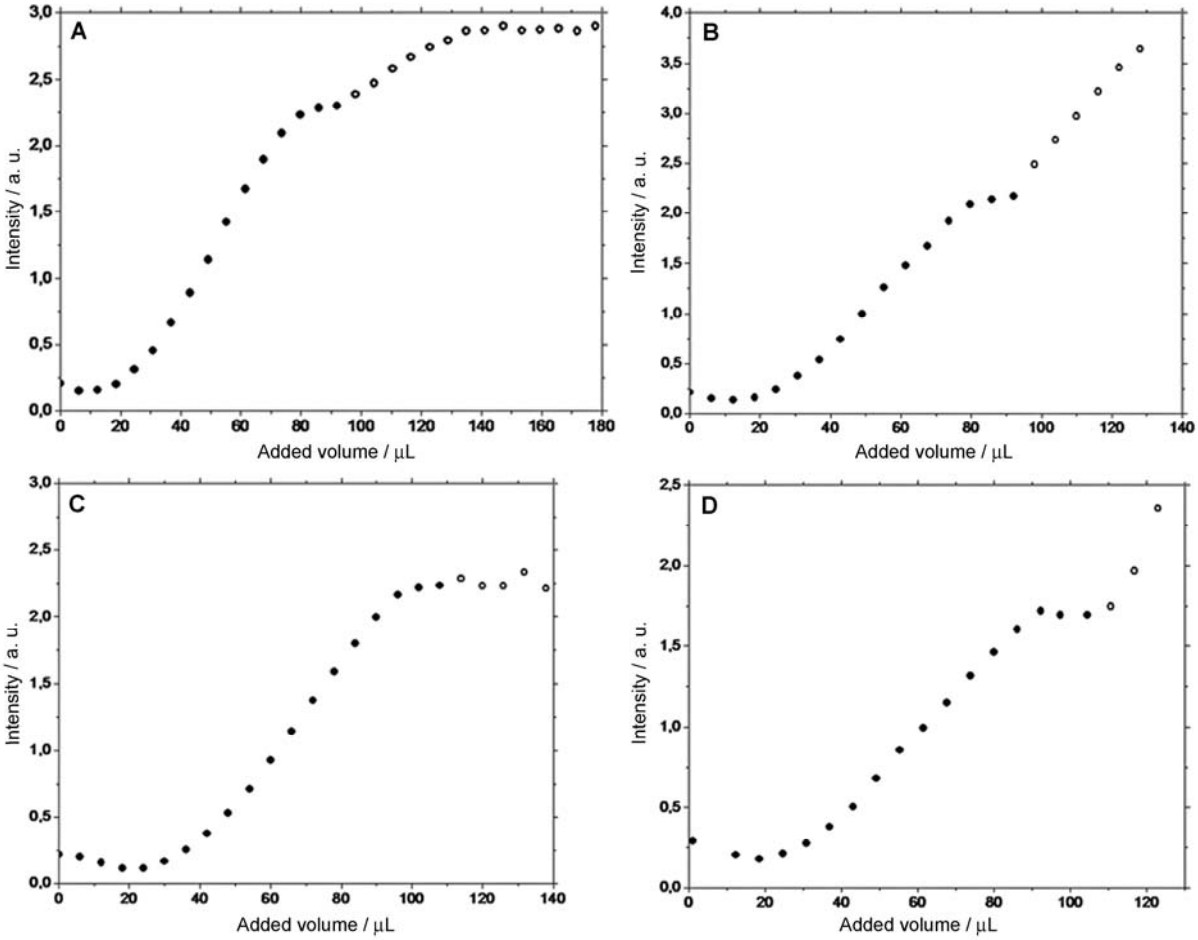

Figure 7. Scattered intensity measured for polymerized PNPs coated with a 400:1 mixture (10 mM and 25 μM, respectively) of **1** and **3** (A, full dots), **1** and **5** (B and C, full dots) and **1** and **4b** (D, full dots), and as a function of the amount of added HSA, (A, empty dots), SAv (B and C, empty dots) and galectin-3 (D, empty dots). A) 20 μM HSA aliquots were added to the solution up to saturation of available maleimido groups (corresponding to the HSA binding sites) on the PnPs. Residual light at the minimum corresponds to point A in Figure 2. B) 50 μM SAv additions were reacted with biotin-containing PnPs, causing interparticle aggregation (no plateau was reached) induced by tetrameric interaction of SAv with biotin. C) 50 μM SAv aliquots were added to **1**-coated PnPs, no aggregation observed. D) 50 μM galectin-3 aliquots were added to PnP dispersion containing lactose functionalities inducing particle aggregation. The experiments were carried out in 5 mM phosphate buffer (pH 7.2) by using a 0.1% (v/v) PnP dispersion.

3. Conclusion

A general and straightforward method for the stable and reliable functionalization of intrinsically unreactive perfluoropolymer nanoparticles was reported, exploiting the coverage of their external surface with newly synthesized unsymmetrical amphiphilic diacetylenes, followed by a clean and safe photopolymerization procedure. Diacetylene molecules were monomerically adsorbed onto our phantom nanoparticles and polymerized by exposure to UV

irradiation. An accurate study of the photopolymerization conditions and of the stability of the resulting polymer shell was performed, the optimal exposure time was assessed and the number/mass of loaded molecules could be sensitively determined. Finally, the potential of the photopolymerization method for the nanoparticle functionalization was demonstrated through the covalent immobilization of a representative protein (HSA). Noteworthy, this light scattering-based method enabled the straightforward measurement of the extent of successful bioconjugation, without the need of complex and time-consuming characterization steps. The applicability of the approach could be further extended by combination with alternative bioconjugation strategies, as demonstrated here with biotin-streptavidin technology and through the detection of the occurrence of reversible carbohydrate-protein interactions. We believe that this strategy can be of wide nanotechnological interest, in view of the outstanding and many-sided, yet still poorly exploited, potential outcomes of perfluorinated materials.

4. Experimental

Materials and Methods: All chemicals were reagent grade and used as supplied from Fluka. Negatively charged perfluorinated spherical copolymer particles (PnPs) were supplied by Solvay Solexis. All reactions were performed in oven-dried glassware under an inert atmosphere (nitrogen or argon) at room temperature unless otherwise noted. Dry pyridine, toluene, *N*,*N*-dimethylformamide, acetonitrile and methanol over molecular sieves were purchased from Fluka and used without further purification. Dichloromethane was freshly distilled from CaH_2 before use. Bovine serum albumin (BSA), Human serum albumin (HSA), human galectin-3, and streptavidin were purchased from Sigma and used as received except galectin-3, which was dialyzed prior to use to remove the lactose stabilizer. Chromatographic purifications were performed by flash chromatography with silica gel 60 (Merck, 40-63 μm eq. 230-400 mesh ASTM) packed in glass columns; the eluting solvent for each purification was determined by thin layer chromatography (TLC). Reactions were monitored by TLC and

HPTLC analysis carried out on Merck silica gel 60 F-254 plates (0.25 mm and 0.2 mm thickness, respectively), and spots were visualized by UV radiation (λ = 254 nm) or by spraying with a 20% solution of sulphuric acid in methanol or with a solution containing ammonium molibdate (21 g) cerium sulphate (1 g), sulphuric acid (31 mL) in 500 mL water, followed by heating at 110 °C for 5 min. ^{1}H NMR and ^{13}C NMR spectra were recorded with a Bruker AVANCE-400 (400 MHz) or with a Bruker AC-300 (300 MHz). Chemical shifts are given in ppm (δ) relative to tetramethylsilane as internal standard. Coupling constants are expressed in Hz. Signals were assigned by means of APT, ^{1}H-^{1}H COSY and ^{1}H-^{13}C HSQC spectra. MALDI-TOF MS experiments were performed in the linear mode on a Bruker Daltonics Microflex LT instrument equipped with a 337 nm nitrogen laser, working with a microSCOUT ion source positioned within the MALDI target. ESI mass spectra were recorded on a Finnigan LCQ Advantage. FTIR analyses of organic monomers were performed on a Nicolet FT-IR Nexux: the sample was dissolved in dichloromethane, deposited between two adjacent NaCl windows and the solvent was allowed to evaporate. FTIR spectra of coated nanoparticles were acquired by ATR measurements on a Varian 670-IR spectrometer equipped with a Specac single-reflection diamond for higher absorption peaks, and by microFTIR on a 610-IR microscope for low absorption peaks. All compounds containing the diacetylene functionality were stored as dichloromethane solutions in the absence of light, in order to avoid uncontrolled polymerization.

Sample Preparation: PnPs were thoroughly dialyzed before use to remove undesired physisorbed byproducts. Despite their hydrophobic character, the purified colloids were stable over several months because of their surface negative electric charges. The particles were dispersed in 5 mM phosphate buffer (pH 7.2) at a volume fraction of $\phi = 10^{-3}$ vol. In all reported experiments surfactants and proteins were added into a cuvette containing 1.5 mL of 0.1% v/v bare PnPs dispersion.

Static Light Scattering: Ninety-degree angle polarized scattered light from a 5-mW He-Ne laser beam was collected and measured with a RCA 931B photomultiplier. We used conventional spectrophotometer cuvettes held in a suitably designed cell holder provided with a ministirrer, the necessary tubing holding, and water flow to control the temperature, in turn measured by a thermistor. Measurements were performed at 30 °C. Diacetylenic surfactants and proteins solutions were injected into the cuvette by motorized pumps (Kent Scientific Genie syringe pump and Ismatec Reglo piston precision pump). Stirring, temperature, and injections were controlled by a computer, through a suitable interface designed ad hoc to program DPS experiments. Experiments were taken by a programmed sequence of injection, stirring, and data acquisition. Typically, each data point is referred to an addition of a few μL of a surfactant or protein solution to the cuvette initially containing 1.5 mL of bare PnPs dispersion. Any injection was typically followed by 10 min of stirring. Sets of 80 independent intensity acquisitions were taken for each condition and analyzed to eliminate possible optical contributions due to dust impurities.

DynamicLlight Scattering: Measurements of the intensity (I) autocorrelation functions were periodically taken to ensure that the PnPs were monomerically dispersed at the various stages of the adsorption curves. The data were taken by using a frequency doubled 532-nm, 150-mW NdYag laser and through a single mode fiber collection of the scattered light. Cross-correlations were calculated with a BI-9000 digital correlator (Brookhaven Instruments Corp.), after the collected I was divided by a 50/50 fiber beam splitter.

Absorbance and Photopolymerization: Absorption spectra were measured in the wavelength range 240-600 nm using a fiber-coupled spectrometer (Ocean Optics Inc., USA). Illumination was provided by fiber-coupled deuterium and halogen lamps. The UV-vis spectra were recorded at 5 min intervals during UV irradiation. Photopolymerization of

samples was promoted by UV laser pulses at 266 nm using a Brilliant laser (Quantel, France) operated with fourth armonic generator. In order to achieve a more uniform illumination of the cuvette, the laser beam was expanded and filtered by means of a diagram with an aperture diameter of 1 cm. The samples were shined with 4 ns pulses with energy of 6-8 mJ each and generated at a repetition rate of 10 Hz, thus delivering an average power of 60-80 mW with a peak power of more than 1 MW.

Acknowledgements

This work was supported by the "Romeo ed Enrica Invernizzi" Foundation, the CNR-Regione Lombardia "Mind in Italy" project, a FIRB grant (CHEM-PROFARMA-NET, RBPR05NWWC) and the Cariplo Foundation. We thank Dr. A. Natalello for help in FT-IR characterization. We are grateful to Solvay Solexis for the generous gift of the perfluorinated colloids and thank M. Bassi for the crucial help in selecting the best polymer composition in the colloid formulation. Supporting Information is available online from Wiley InterScience or from the author.

Received: ((will be filled in by the editorial staff))
Revised: ((will be filled in by the editorial staff))
Published online: ((will be filled in by the editorial staff))

[1] M. P. Krafft, J. G. Riess, *J. Polym. Sci. Pol. Chem.* **2007**, *45*, 1185.

[2] J. E. Puskas, Y. H. Chen, *Biomacromolecules* **2004**, *5*, 1141.

[3] A. Ghetta, D. Prosperi, F. Mantegazza, L. Panza, S. Riva, T. Bellini, *Proc. Natl. Acad. Sci. U. S. A.* **2005**, *102*, 15866.

[4] D. Prosperi, C. Morasso, F. Mantegazza, M. Buscaglia, L. Hough, T. Bellini, *Small* **2006**, *2*, 1060.

[5] D. Prosperi, C. Morasso, P. Tortora, D. Monti, T. Bellini, *ChemBioChem* **2007**, *8*, 1021.

[6] C. Morasso, T. Bellini, D. Monti, M. Bassi, D. Prosperi, S. Riva, *ChemBioChem* **2009**, *10*, 639.

[7] M. Mammen, S.-K. Choi and G. M. Whitesides, Angew. Chem. Int. Ed. **1998**, *37*, 2754.

[8] M. A. N. Coelho, E. P. Vieira, H. Motschmann, H. Mohwald, A. F. Thunemann, *Langmuir* **2003**, *19*, 7544.

[9] C. E. Giacomelli, W. Norde, *Biomacromolecules* **2003**, *4*, 1719.

[10] S. H. Mollmann, J. T. Bukrinsky, S. Frokjaer, U. Elofsson, *J. Colloid Interface Sci.* **2005**, *286*, 28.

[11] J. Vörös, *Biophys. J.* **2004**, *87*, 553.

[12] C. M. Santos, A. Kumar, W. Zhang, C. Cai, *Chem. Commun.* **2009**, 2854.

[13] C.-A. J. Lin, R. A. Sperling, J. K. Li, T.-Y. Yang, P.-Y. Li, M. Zanella, W. H. Chang, W. J. Parak, *Small* **2008**, *4*, 334.

[14] S.-W. Kim, S. Kim, J. B. Tracy, A. Jasanoff, M. G. Bawendi, *J. Am. Chem. Soc.* **2005**, *127*, 4556.

[15] M. S. Nikolic, M. Krack, V. Aleksandrovic, A. Kornowski, S. Förster, H. Weller, *Angew. Chem. Int. Ed* **2006**, *45*, 6577.

[16] R. A. Sperling, T. Pellegrino, J. K. Li, W. H. Chang, W. J. Parak, *Adv. Funct. Mater.* **2006**, *16*, 943.

[17] Y. Lu, Y. Yang, A. Sellinger, M. Lu, J. Huang, H. Fan, R. Haddad, G. Lopez, A. R. Burns, D. Y. Sasaki, J. Shelnutt, C. J. Brinker, *Nature* **2001**, *410*, 913.

[18] R. Jelinek, S. Kolusheva, in *Creative Chemical Sensor Systems*, vol. 277, (Ed: Editon), Springer-Verlag Berlin, Berlin, Germany **2007**, pp. 155.

[19] M. A. Reppy, B. A. Pindzola, *Chem. Commun.* **2007**, 4317.

[20] X. Y. Zhang, F. H. Chen, J. Z. Ni, *Drug Deliv.* **2009**, *16*, 280.

[21] W. Jiang, S. Mardyani, H. Fischer, W. C. W. Chan, *Chem. Mater.* **2006**, *18*, 872.

[22] S. I. Kasteren, S. J. Campbell, S. Serres, D. C. Anthony, N. R. Sibson, B. G. Davis, *Proc. Natl. Acad. Sci. U. S. A.* **2009**, *106*, 18.

[23] H. C. Kolb, M. G. Finn, K. B. Sharpless, *Angew. Chem. Int. Ed.* **2001**, *40*, 2004-2021.

[24] M. Meldal, C. W. Tornoe, *Chem. Rev.* **2008**, *108*, 2952.

[25] M. Fleiner, P. Benzinger, T. Fichert, U. Massing, *Bioconjugate Chem.* **2001**, *12*, 470.

[26] S. F. Schluter, P. L. Ey, *J. Immunol. Methods* **1984**, *66*, 89.

[27] P. Charley, P. Saltman, *Science* **1963**, *139*, 1205.

[28] N. M. Green, *Adv. Protein Chem.* **1975**, *29*, 85.

[29] N. M. Green, *Biochem. J.* **1963**, *89*, 609.

[30] M. N. Khan, *J. Org. Chem.* **2002**, *60*, 4536.

[31] L. Polito, D. Monti, E. Caneva, E. Delnevo, G. Russo, D. Prosperi, *Chem. Commun.* **2008**, 621.

[32] R. Schmidt, R., J. Michel, *Angew. Chem. Int. Ed.* **1980**, *19*, 731.

[33] M. Wenzel, G. H. Atkinson, *J. Am. Chem. Soc.* **1989**, *111*, 6123.

[34] R. R. Chance, *Macromolecules* **1980**, *13*, 396.

Submitted to ADVANCED FUNCTIONAL MATERIALS

A smart method for the biofunctionalization of strongly inert perfluoropolymer nanoparticles (PnPs) is presented, via stable coating with novel diacetylenic compounds followed by clean UV photopolymerization to generate reactive functionalities on PnP surface. This method further allows for the fine tuning of the amount of conjugated biomolecules, which can be sensitively and straightforwardly quantified.

Keyword: Colloids; Perfluoropolymer; Functional coating; Surface modification; Photochemistry

C. Morasso, M. Colombo, S. Ronchi, L. Polito, D. Monti, M. Buscaglia, T. Bellini, D. Prosperi*

Towards a Universal Method for the Stable and Clean Functionalization of Inert Perfluoropolymer Nanoparticles: Exploiting Photopolymerizable Amphiphilic Diacetylenes

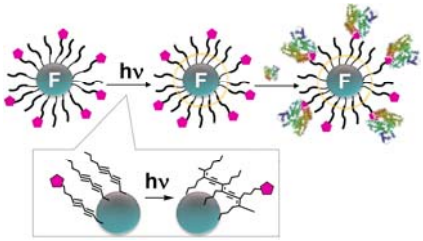

Supporting Information

Synthesis of 3,6,9,12,15-pentaoxaheptadecan-1,17-diol-1-benzoate (15)

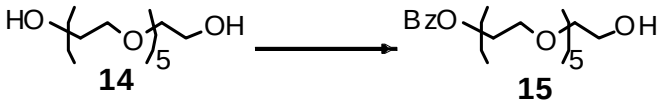

Hexaethylene glycol **14** (1 g, 3.5 mmol) was dried under vacuum for 1 h. The compound was dissolved in dry CH_2Cl_2 (15 mL) and triethylamine (535 µL, 3.8 mmol) was added. The solution was cooled to 0 °C and benzoyl chloride (404 µL, 3.5 mmol) was added portionwise. After 1 h the reaction mixture was allowed to warm to room temperature and stirred overnight. Solvents were evaporated under reduced pressure and the residue was purified by silica gel chromatography (EtOAc) affording product **15** (640 mg, 1.6 mmol, 48%) as colorless oil. The product was used without further characterization. Spectra were consistent with previously reported data.[1]

Synthesis of 17-azido-3,6,9,12,15-pentaoxaheptadecan-1-ol (7a)

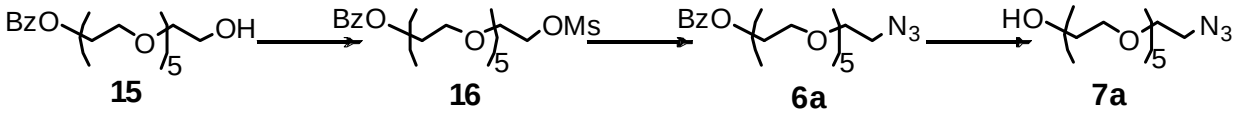

Compound **15** (640 mg, 1.6 mmol) was dissolved in dry CH_2Cl_2 (10 mL). Triethylamine (350 µL, 2.5 mmol) was added, followed by methanesulfonyl chloride (173 µL, 2.2 mmol), then the mixture was stirred for 2.5 h. The reaction mixture was washed with water and the organic phase was dried over Na_2SO_4. The solvent was removed under reduced pressure affording the mesylate **16** as a yellow oil. The crude product **16** was dissolved in a 20% w/w NaN_3/water solution (2.5 mL), in the presence of tetrabutylammonium bromide (25 mg, 0.08 mmol) and the mixture was heated to reflux for 2 h. The disappearance of the starting material was followed by TLC (EtOAc). The mixture was diluted with water, then extracted with CH_2Cl_2.

The combined organic phases were dried over Na_2SO_4 and the solvent was removed under reduced pressure. The product was purified by a silica gel filtration (EtOAc), leading to product **6a** in quantitative yield (650 mg, 1.6 mmol). Compound **6a** (2.0 g, 4.9 mmol) was dissolved in dry MeOH (10 mL). A solution of MeONa (1 M in MeOH, 2.4 mL, 2.4 mmol) was added dropwise and the mixture was stirred for 3 h. The reaction was quenched by addition of Amberlite resin until pH ≈ 7 and the solvent was removed under vacuum. The crude product was purified by silica gel chromatography (EtOAc/MeOH 9/1), affording product **7a** (1.28 g, 4.17 mmol, 85%) as colorless oil. Spectra were consistent with previously reported data.[2]

Synthesis of 17-amino-3,6,9,12,15-pentaoxaheptadecan-1-ol (17)

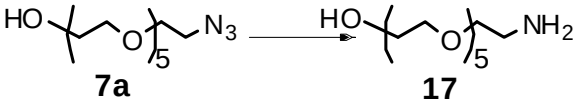

7a **17**

Compound **7a** (350 mg, 1.1 mmol) was dissolved in dry MeOH (15 mL). A catalytic amount of Pd/C was added to the solution, under H_2 atmosphere. The reaction mixture was stirred for 3 h at room temperature. The suspension was then filtered on a Celite® pad and the solvents were removed under vacuum, affording compound **17**. ^{1}H NMR signals were consistent with those reported in ref.[3] No further purification of product **17** was required and it was directly used for the next reaction.

Synthesis of *N*-(17-hydroxy-3,6,9,12,15-pentaoxaheptadecyl) 5,7-hexadecadiynamide (1)

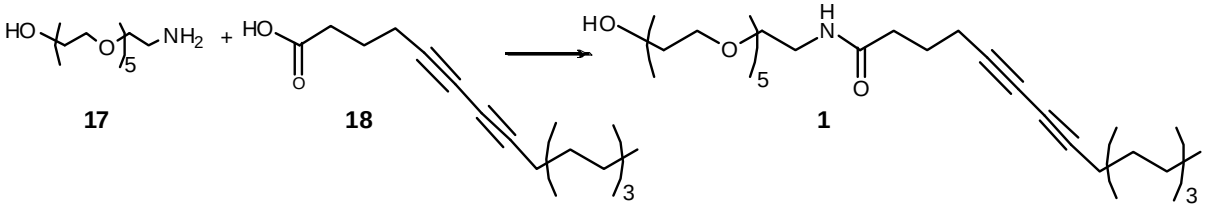

17 **18** **1**

5,7-Hexadecadiynoic acid **18** (321 mg, 1.3 mmol) was dissolved in CH_2Cl_2. The mixture was filtered to remove the polymerized portion and the solvents were removed under vacuum. The

acid **18** was then dissolved in dry CH_2Cl_2 (15 mL) and NHS (230 mg, 2 mmol) was added. The reaction mixture was cooled to 0 °C and DCC (383 mg, 1.86 mmol) was added. The solution was stirred for 2 h and slowly warmed to room temperature. A solution of compound **17** (303 mg, 1.08 mmol) in dry CH_2Cl_2 (1 mL) was added to the reaction mixture, immediately followed by triethylamine (400 µL, 5.4 mmol). The mixture was stirred overnight at room temperature, then it was filtered and the solvents were removed in vacuum. The crude product was dissolved in a 1 M HCl solution and filtered. The aqueous layer was extracted with CH_2Cl_2 and the combined organic phases were dried over Na_2SO_4, filtered, concentrated under reduced pressure and purified via flash chromatography (EtOAc/MeOH 8/2) leading to compound **1** (160 mg, 0.3 mmol, 25%).

^{1}H NMR (400 MHz, $CDCl_3$): δ = 6.65 (br s, 1H, CON*H*), 3.73-3.54 (m, 24H, OCH_2CH_2O), 3.44 (m, 2H, CH_2NHCO), 3.38 (br s, 2H, CH_2CH_2OH), 2.31 (m, 4H, CH_2-C≡C-C≡C-CH_2), 2.23 (t, *J* = 7.0 Hz, 2H, CH_2CONH), 1.85 (q, *J* = 7.0 Hz, 2H, C$H_2$$CH_2$CONH), 1.49 (q, *J* = 7.2 Hz, 2H, C$H_2$$CH_2$C≡), 1.40-1.27 (m ,10H, 5 CH_2), 0.88 (t , *J* = 7.0 Hz, 3H, CH_2CH_3); ^{13}C NMR (100 MHz, $CDCl_3$): δ = 172.32, 77.83, 76.45, 72.61, 70.45, 70.15, 70.10, 69.92, 66.03, 65.21, 61.57, 39.23, 35.02, 31.80, 29.12, 29.04, 28.85, 28.33, 24.21, 22.62, 19.17, 18.77, 14.07; MALDI-MS (*m*/*z*) calcd for $C_{28}H_{49}NO_7Na$, 534.3; found, 534.1. Anal. calcd for $C_{28}H_{49}NO_7$: C, 65.72; H, 9.65; N, 2.74; found: C, 65.82; H, 9.64; N, 2.75.

Synthesis of 1-oxo-1-phenyl-2,5,8,11-tetraoxatridecan-13-ol (20)

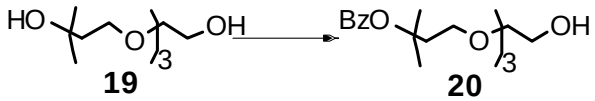

19 **20**

Tetraethylene glycol **19** (10.0 g, 52 mmol) was dried under vacuum for 1 h. The oil was dissolved in dry CH_2Cl_2 (40 mL) and cooled to 0 °C. Triethylamine (8.6 mL, 63 mmol) was added, followed by benzoyl chloride (7.3 g, 52 mmol). The reaction was stirred for 1 h, then warmed to room temperature and stirred overnight. The mixture was diluted with CH_2Cl_2 and

washed with water. The organic layers were dried over Na_2SO_4 and the solvent was removed under vacuum. The product was purified by silica gel filtration (hexanes/EtOAc 1/9), leading to product **20** (5.8 g, 20.8 mmol, 40%). Spectra were consistent with previously reported data.[1]

Synthesis of 11-azido-3,6,9-trioxaundecanol (7a)

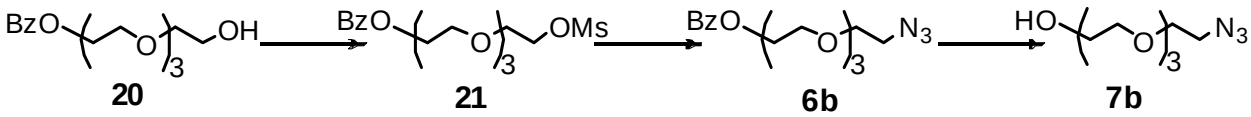

To a solution of compound **20** (5.6 g, 18.8 mmol) in dry CH_2Cl_2 (40 mL), triethylamine (3.9 mL, 28 mmol) was added, followed by methanesulfonyl chloride (2.0 mL, 26.3 mmol). The reaction mixture was stirred for 2 h, then washed with water. The organic phase was dried over Na_2SO_4 and the solvent was removed under reduced pressure, affording the product **21** as yellow oil. The crude product **21** was dissolved in a 20% w/w NaN_3/water solution (7.5 mL) in the presence of tetrabutylammonium bromide (275 mg, 0.8 mmol) and heated to reflux for 75 min. The disappearance of the starting material and the formation of the azide **6b** were followed by TLC (EtOAc). The mixture was diluted with water and extracted with CH_2Cl_2. The combined organic phases were dried over Na_2SO_4 and the solvents were removed under vacuum. The product was purified by silica gel filtration (EtOAc), affording product **6b** (5.8 g, 17.9 mmol, 95%). Compound **6b** (5.7 g, 17.6 mmol) was dissolved in dry MeOH (10 mL). A solution of MeONa (1 M, 3.5 mL, 3.5 mmol) was added dropwise and the mixture was stirred overnight. The reaction was quenched by addition of Amberlite resin until pH ≈ 7 and the solvent was removed under vacuum. The crude product was purified by silica gel chromatography (EtOAc), affording product **7b** (3.0 g, 13.7 mmol, 80%) as colorless oil. Spectra were consistent with previously reported data.[4]

Synthesis of 2-(11-azido-3,6,9-trioxaundecyl)-4,5,6,7-tetrachloro-1*H*-isoindole-1,3(2*H*)-dione (22)

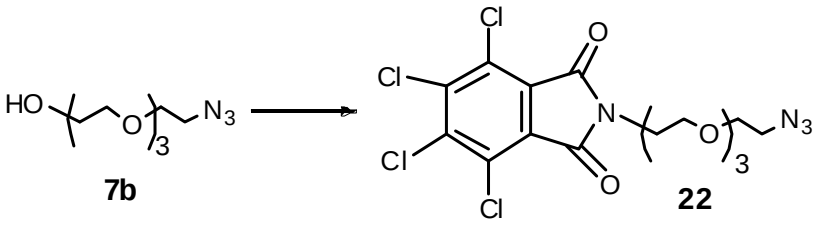

Freshly crystallized triphenylphosphine (1.29 g, 4.1 mmol) and tetrachloro phtalimide (1.12 g, 4.9 mmol) were dissolved in 18 mL of dry THF and cooled to –78 °C. Di-*t*-butyl-azodicarboxylate (1.13 g, 4.9 mmol) was dissolved in 3 mL of dry THF and added dropwise to the reaction mixture. After 15 min a solution of compound **7b** (900 mg, 4.1 mmol) in dry THF (3 mL) was added and the reaction mixture was allowed to warm to room temperature and stirred overnight. The solvent was removed under vacuum and the crude product was purified by silica gel chromatography (hexanes/EtOAc 1/1), affording product **22** (1.5 g, 3 mmol, 75%) as a white solid.

^{1}H NMR (400 MHz, $CDCl_3$): δ = 3.91 (t, *J* = 5.6 Hz, 2H, OCH_2CH_2NPht), 3.75 (t, *J* = 5.6 Hz, 2H, OCH_2CH_2NPht), 3.66-3.62 (m, 10H, 5 OCH_2), 3.37 (t, *J* = 5.2 Hz, 2H, $OCH_2CH_2N_3$); ^{13}C NMR (100 MHz, $CDCl_3$): δ = 162.42, 140.01, 129.60, 127.68, 70.67, 70.11, 70.03, 67.44, 50.68, 38.09; MALDI-MS [M-2N+2H] (*m*/*z*) calc. for $C_{16}H_{18}Cl_4N_2O_5$, 460.1; found, 460.0. Anal. calcd for $C_{16}H_{16}Cl_4N_4O_5$: C, 39.53; H, 3.32; N, 11.52; found: C, 39.59; H, 3.32; N, 11.49.

Synthesis of 11-Azido, 3,6,9-trioxaundecan-1-amine (8)

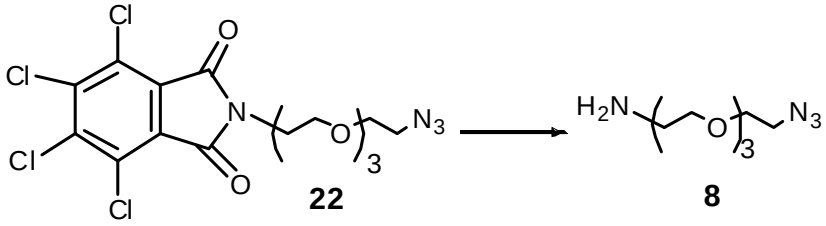

Compound **22** (400 mg, 0.82 mmol) was suspended in EtOH (10 mL). The mixture was warmed to 35 °C, hydrazine monohydrate (100 µL, 2.8 mmol) was added and the suspension

was heated to reflux for 3 h. The solvent was evaporated under reduced pressure and the residue was dissolved in CH_2Cl_2 and washed three times with a 5% solution of NaOH. The organic phase was dried over Na_2SO_4 and the solvent was removed under vacuum. The crude product **8** was used without further characterization. Spectra were consistent with previously reported data.[5]

Synthesis of *N*-(11-azido, 3,6,9-trioxaundecyl) 5,7-hexadecadiynamide (2)

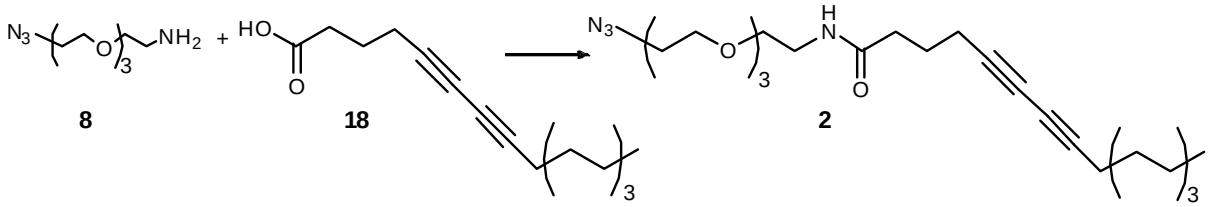

Compound **8** (300 mg, 1.4 mmol) was dissolved in dry DMF (15 mL) followed by *N*,*N*-diisopropyl ethylamine (500 µl, 2.8 mmol) and 5,7-hexadecadiynoic acid **18** (321 mg, 1.3 mmol). After 10 min, the solution was cooled to 0 °C and PyBOP (730 mg, 1.4 mmol) was added. The reaction mixture was stirred for 72 h, the solvent was removed under vacuum and the crude product was purified by silica gel chromatography (EtOAc), affording product **2** (290 mg, 3 mmol, 46%) as colorless oil.

^{1}H NMR (400 MHz, $CDCl_3$): δ = 6.09 (s, 1H, CON*H*), 3.71-3.64 (m, 10H, 5 OCH_2), 3.57 (t, *J* = 5.2 Hz, 2H, CH_2CH$_2$NHCO), 3.44 (t, *J* = 5.2 Hz, 2H, CH_2NHCO), 3.40 (t, *J* = 4.8 Hz, 2H, CH_2N$_3$), 2.35 (m, 4H, CH_2-C≡C-C≡C-CH_2), 2.25 (t, *J* = 6.8 Hz, 2H, CH_2CONH), 1.87 (q, *J* =7.0 Hz, 2H, CH_2CH$_2$CONH), 1.52 (m, 2H, CH_2CH$_2$C≡), 1.44-1.27 (m, 10H, 5 CH_2), 0.89 (t, *J* = 6.6 Hz, 3H, CH$_2$CH_3); ^{13}C NMR (100 MHz, $CDCl_3$): δ = 172.08, 77.98, 76.28, 70.75, 70.64, 70.30, 70.09, 69.86, 69.11, 66.16, 65.14, 50.70, 39.22, 35.08, 31.83, 29.15, 29.07, 28.88, 24.10, 22.65, 19.20, 18.71, 14.11; MALDI-MS (*m*/z) calcd for $C_{24}H_{40}N_4O_4Na$, 471.3; found, 470.1. Anal. calcd for $C_{24}H_{40}N_4O_4$: C, 64.26; H, 8.99; N, 12.49; found: C, 64.16; H, 9.00; N, 12.46.

Synthesis of 1-(3,6,9,12-tetraoxapentadec-14-ynyl)-1*H*-pyrrole-2,5-dione (10)

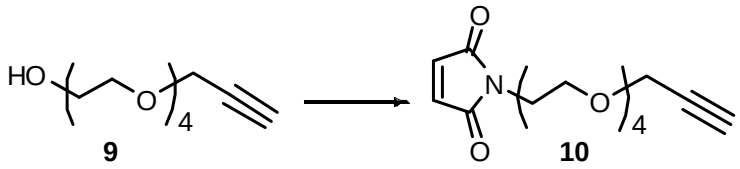

9 **10**

Propargyl tetraethylene glycol **9**[6] (300 mg, 1.37 mmol) and polymer-bound triphenylphosphine (430 mg, 1.64 mmol) were dissolved in dry THF (20 mL). The reaction mixture was cooled to -78 °C and a solution of di-*t*-butyl-azodicarboxylate (337 mg, 1.64 mmol) in dry THF (3 mL) was added dropwise. After 10 min a solution of maleimide (133 mg, 1.37 mmol) in dry THF (3 mL) was added. The mixture was stirred for 2.5 h, then polymer-bound triphenylphosphine oxide was filtered and the solvent was removed under reduced pressure. Compound **10** (210 mg, 0.67 mmol, 49%) was purified via silica flash chromatography (EtOAc/hexanes 9/1).

^{1}H NMR (400 MHz, $CDCl_3$): δ = 6.66 (s, 2H, *H*C=C*H*), 4.14 (d, *J* = 2.4 Hz, 2H, OC*H*$_2$C≡CH), 3.67-3.51 (m, 16H, 8 C*H*$_2$) 2.41 (t, *J* = 2.4 Hz, 1H, $OCH_2C{\equiv}CH$); ^{13}C NMR (100 MHz, $CDCl_3$): δ = 170.60, 134.14, 79.60, 74.58, 70.53, 70.32, 70.00, 69.06, 67.73, 58.30, 37.09; ESI-MS (*m*/*z*) calcd for $C_{15}H_{21}NO_6Na$, 334.1; found, 334.1. Anal. calcd for $C_{15}H_{21}NO_6$: C, 57.87; H, 6.80; N, 4.50; found: C, 57.78; H, 6.79; N, 4.49.

Synthesis of 3,6,9,12-tetraoxapentadec-14-ynyl-(2',3',4',6'-tetra-*O*-acetyl-β-D-galactopyranosyl)-(1→4)-2,3,6-tri-*O*-acetyl-β-D-glucopyranoside (11)

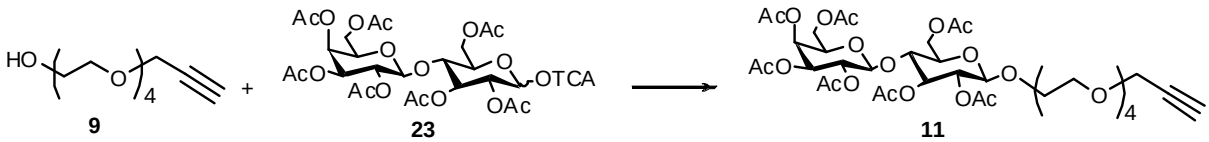

9 **23** **11**

Compound **23**[7] (144 mg, 0.18 mmol) and propargyl tetraethylene glycol **9** (86 mg, 0.37 mmol) were dried under vacuum overnight. The compounds were dissolved in dry CH_2Cl_2 (5 mL) and the solution was cooled to –30 °C. A solution of trimethylsilyltriflate (0.29 mL, 1 M

in dry CH_2Cl_2) was added dropwise and the solution was allowed to warm to room temperature. The mixture was stirred for 2 h under a nitrogen atmosphere, then the reaction was quenched by addition of triethylamine. The solvent was removed under reduced pressure and the product was purified by silica gel chromatography (hexanes/EtOAc 1/1), yielding compound **11** (140 mg, 0.16 mmol, 89%) as colorless oil. Spectra were consistent with previously reported data.[8]

Synthesis of 2-(3,6,9,12-tetraoxapentadec-14-ynyl)-4,5,6,7-tetrachloro-1*H*-isoindole-1,3(2*H*)-dione (24)

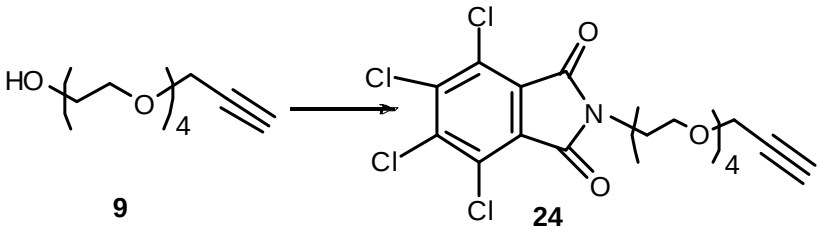

9 **24**

Propargyl tetraethylene glycol **9** (300 mg, 1.29 mmol) was dissolved in dry THF (12 mL), then Ph_3P (370 mg, 1.42 mmol) and tetrachlorophthalimide (370 mg, 1.29 mmol) were added. A solution of di-*t*-butylazadicarboxylate (330 mg, 1.42 mmol) in dry THF (3 mL) was slowly added and the mixture was stirred at room temperature for 3 h. The reaction was monitored by TLC (hexanes/EtOAc 1/1). The mixture was quenched with water, diluted with dichloromethane and dried over Na_2SO_4. The crude product was purified by silica gel flash chromatography (hexanes/EtOAc 1/1), yielding **24** (480 mg, 0.96 mmol, 75%) as a yellowish solid. Spectra were consistent with previously reported data.[8]

Synthesis of 3,6,9,12-tetraoxapentadec-14-yn-1-amine (12)

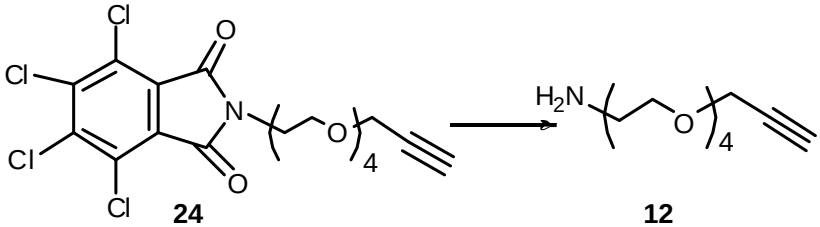

24 **12**

Product **24** (100 mg, 0.20 mmol) was suspended in EtOH (5 mL). The reaction mixture was warmed to 35 °C, hydrazine monohydrate (25 µL, 0.7 mmol) was added and the suspension was heated to reflux for 3 h. The solvent was evaporated under reduced pressure and the residue was dissolved in CH_2Cl_2 and washed three times with a 5% solution of NaOH. The organic phase was dried over Na_2SO_4 and the solvent was removed under vacuum. The crude product **12** was used without further characterization.[8]

Synthesis of 5-((3a*S*,4*S*,6a*R*)-2-oxohexahydro-1*H*-thieno[3,4-*d*]imidazol-4-yl)-*N*-(3,6,9,12-tetraoxapentadec-14-ynyl)pentanamide (13)

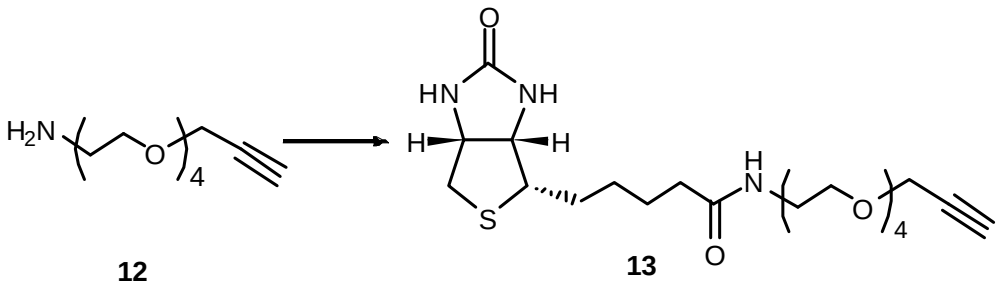

12 **13**

Compound **12** (300 mg, 1.29 mmol), biotin (316 mg, 1.19 mmol) and DIPEA (450 µl, 2.59 mmol) were dissolved in dry DMF (5 mL). After 10 min PyBOP was added and the mixture was stirred for 24 h. The solvent was removed under reduced pressure and the crude product was purified by silica gel flash chromatography (CH_2Cl_2/MeOH 95/5) affording product **13** (210 mg, 0.47 mmol, 36%) as colorless oil.

^{1}H NMR (400 MHz, $CDCl_3$): δ = 6.82 (t, *J* = 5.6 Hz, 1H, CON*H*), 6.65 (br s, 1H , N*H*CONH), 5.73 (s, 1H, NHCON*H*), 4.50 (m, 1H, NHCONH-C*H*), 4.32 (m, 1H, C*H*-NHCONH), 4.20 (d, *J* = 2.4 Hz, 2H, OCH_2C≡CH), 3.68-3.57 (m, 14H, 7 OCH_2), 3.43 (m, 2H, OCH_2), 3.14 (m, 1H, CH_2SC*H*), 2.90 (dd, *J* = 4.8 Hz, *J* = 12.8 Hz, 1H, CH_aH$_b$SCH), 2.74 (d, *J* = 12.8 Hz, 1H, CH$_a$*H*$_b$SCH), 2.46 (t, *J* = 2.4 Hz, 1H, OCH$_2$C≡C*H*), 2.24 (t, *J* =7.6 Hz, 2H, CH_2CONH), 1.80-1.60 (m, 4H, 2 CH_2), 1.49-1.41 (m, 2H, CH_2);^{13}C NMR (100 MHz, $CDCl_3$): δ = 173.36, 164.14, 80.00, 74.65 70.59, 70.40, 70.11, 69.99, 69.13, 61.80, 60.24, 58.40, 55.66, 40.53,

39.18, 35.99, 28.26, 28.13, 25.62; ESI-MS (*m*/*z*) calcd for $C_{21}H_{35}N_3O_6SNa$, 480.2; found, 480.5. Anal. calcd for $C_{21}H_{35}N_3O_6S$: C, 55.12; H, 7.71; N, 9.18; found: C, 55.20; H, 7.73; N, 9.17.

Synthesis of *N*-(11-(4-(13-(2,5-dioxo-2,5-dihydro-1*H*-pyrrol-1-yl)-2,5,8,11-tetraoxatridecyl)-1*H*-1,2,3-triazol-1-yl)-3,6,9-trioxaundecyl)-5,7-hexadecadiynamide (3)

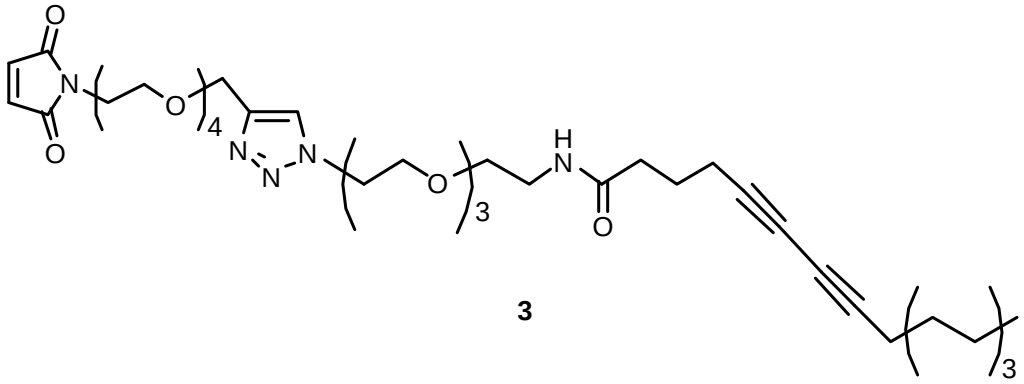

3

Compound **10** (33 mg, 0.1 mmol), $CuSO_4 \cdot 5H_2O$ (4.8 mg, 0.02 mmol) and Na ascorbate (9.9 mg, 0.05 mmol) were dissolved in water (4 mL). Product **2** (50 mg, 0.11 mmol) was dissolved in CH_2Cl_2 (1 mL), and added to the water solution giving a biphasic mixture. The reaction mixture was stirred for 3 h at room temperature, then water and CH_2Cl_2 were added. The organic layer was recovered, dried over Na_2SO_4 and the solvent was evaporated under reduced pressure. The crude product was purified by silica gel flash chromatography (CH_2Cl_2/MeOH 95/5) affording product **3** (60 mg, 0.079 mmol, 79%) as colorless oil. ^{1}H NMR (400 MHz, $CDCl_3$): δ = 7.77 (s, 1H, C*H* triazole), 6.61 (s, 2H, *HC*=C*H*), 6.21 (br s, 1H, CON*H*), 4.69 (s, 2H, OC*H*$_2$C-triazole), 4.55 (t, *J* = 4.8 Hz, 2H, triazole-N-C*H*$_2$), 3.90 (t, *J* = 4.8 Hz, 2H, triazole-N-CH$_2$-C*H*$_2$O), 3.74-3.54 (m, 26H, 13 OC*H*$_2$), 3.44 (t, *J* = 5.2 Hz, 2H, C*H*$_2$NHCO), 2.33 (m, 4H, C*H*$_2$-C≡C-C≡C-C*H*$_2$), 2.24 (t, *J* = 6.8 Hz, 2H, NHCOC*H*$_2$), 1.86 (q, *J* =7.0 Hz, 2H, NHCOCH$_2$C*H*$_2$), 1.52 (m, 2H, C*H*$_2$CH$_2$C≡), 1.38-1.28 (m, 10H, 5 C*H*$_2$), 0.89 (t, *J* = 7.2 Hz, 3H C*H*$_3$); ^{13}CNMR (100 MHz, $CDCl_3$): δ = 172.13, 170.64, 144.91, 134.16, 123.83, 77.98, 76.35, 70.54, 70.22, 70.06, 69.87, 69.69, 69.48, 69.14, 67.81, 66.14, 65.16, 64.62, 50.23, 39.21, 37.15, 35.05, 31.81, 29.13, 29.05, 28.87, 28.33, 24.14, 22.63, 19.18,

18.72, 14.08; MALDI-MS (*m/z*) calcd for $C_{39}H_{61}N_5O_{10}$, 759,4; found, 759.9. Anal. calcd for $C_{39}H_{61}N_5O_{10}$: C, 61.64; H, 8.09; N, 9.22; found: C, 61.55; H, 8.07; N, 9.20.

Synthesis of *N*-(11-(4-(13-(2',3',4',6'-tetra-*O*-acetyl-β-D-galactopyranosyl-(1→4)-2,3,6-tri-*O*-acetyl-β-D-glucopyranosyloxy)-2,5,8,11-tetraoxatridecyl)-1*H*-1,2,3-triazol-1-yl)-3,6,9-trioxaundecyl)-5,7-hexadecadiynamide (4a)

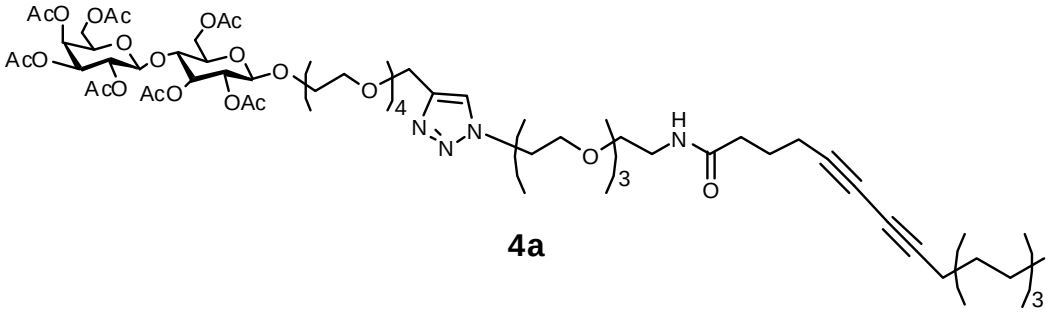

4a

Compound **11** (85 mg, 0.1 mmol), $CuSO_4 \cdot 5H_2O$ (4.8 mg ,0.02 mmol) and Na ascorbate (9.8 mg, 0.05 mmol) were dissolved in water (4 mL). Product **2** (50 mg, 0.11 mmol) was dissolved in CH_2Cl_2 (1 mL), and added to the water solution giving a biphasic mixture. The reaction mixture was stirred for 3 h at room temperature, then water and CH_2Cl_2 were added. The organic layer was recovered, dried over Na_2SO_4 and the solvent was evaporated under reduced pressure. The crude product was purified by silica gel flash chromatography (CH_2Cl_2/MeOH 95/5) affording product **4a** (55 mg, 0.071 mmol, 71%) as colorless oil.

^{1}H NMR (400 MHz, $CDCl_3$): δ = 7.77 (s, 1H, C*H* triazole), 6.21 (br s, 1H, CON*H*), 5.34 (br d, $J_{3',4'}$ = 3.4 Hz, 1H, H-4'), 5.18 (t, $J_{2,3} = J_{3,4}$ = 9.3 Hz, 1H, H-3), 5.10 (dd, $J_{1',2'}$ = 7.9, $J_{2',3'}$ = 10.4 Hz, 1H, H-2'), 4.95 (dd, $J_{2',3'}$ = 10.4, $J_{3',4'}$ = 3.4 Hz, 1H, H-3'), 4.88 (dd, $J_{2,3}$ = 9.3, $J_{1,2}$ = 8.0 Hz, 1H, H-2), 4.68 (s, 2H, OCH_2C-triazole), 4.55 (m, 3H, triazole-N-CH_2, H-1), 4.50-4.46 (m, 2H, H-6a, H-1'), 4.15-4.05 (m, 3H, H-6b, H-6'a, H-6'b), 3.91 (m, 3H, triazole-N-CH_2-CH_2O, H-5'), 3.79 (t, $J_{3,4}$ = 9.3 Hz, 1H, H-4), 3.73-3.60 (m, 25H, 12 OCH_2 and H-5), 3.55 (t, 2H, *J* = 5.2 Hz, OCH_2CH$_2$NHCO), 3.43 (m, 2H, OCH$_2$CH_2NHCO), 2.34-2.22 (m, 6H, CH_2-C≡C-C≡C-CH_2 and NHCOCH_2), 2.15 (s, 3H, COCH_3), 2.11 (s, 3H, COCH_3), 2.06-2.03 (m, 12H, 4 COCH_3), 1.96 (s, 3H, COCH_3), 1.86 (q, *J* =7.2 Hz, 2H, NHCOCH$_2$CH_2), 1.51 (m, 2H,

CH_2CH$_2$C≡), 1.36-1.24 (m, 10H, 5 CH_2), 0.88 (t, J = 6.4 Hz, 3H, CH_3); ^{13}C NMR (100 MHz, $CDCl_3$): δ = 172.10, 170.29, 170.08, 169.98, 169.69, 169.59, 169.02, 144.87, 128.28, 101.05, 100.63, 77.94, 76.27, 72.84, 72.64, 70.99, 70.55, 70.20, 69.83, 69.67, 69.43, 69.15, 69.07, 66.65, 66.14, 65.18, 64.54, 62.04, 60.80, 50.28, 39.19, 35.03, 31.78, 29.65, 29.09-28.84, 28.31, 24.13, 22.60, 20.80, 20.58, 20.45, 19.15, 18.70, 14.05; MALDI-MS (*m*/*z*) calcd for $C_{61}H_{94}N_4O_{26}Na$, 1321.6; found, 1321.1. Anal. calcd for $C_{61}H_{94}N_4O_{26}$: C, 56.38; H, 7.29; N, 4.31; found: C, 56.30; H, 7.28; N, 4.30.

Synthesis of (3a*S*,4*S*,6a*R*)-*N*-(1-(1-(13-oxo-3,6,9-trioxa-12-azaoctacosa-17,19-diynyl)-1*H*-1,2,3-triazol-4-yl)-2,5,8,11-tetraoxatridecan-13-yl)-hexahydro-2-oxo-1*H*-thieno-[3,4-*d*]imidazole-4-pentanamide (5)

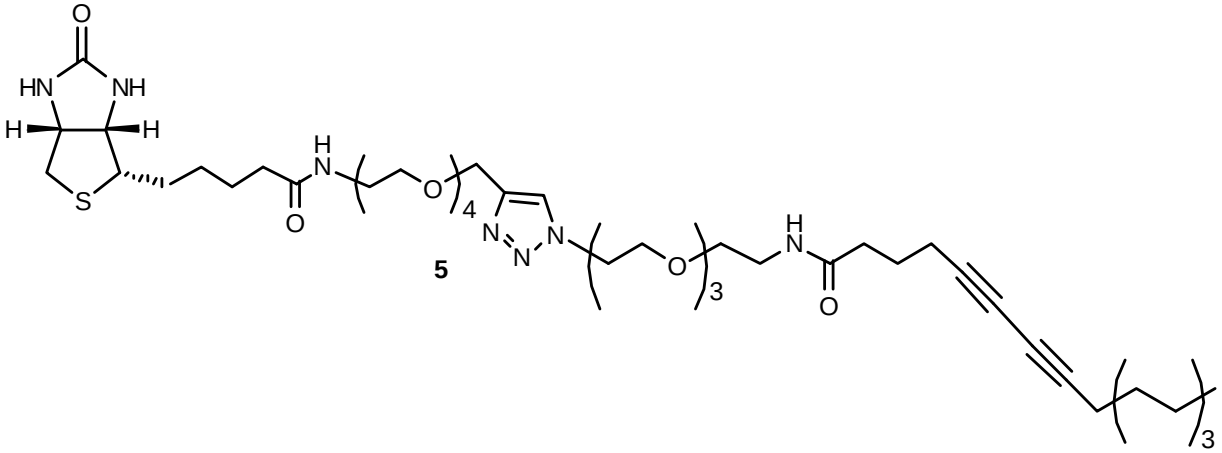

Compound **2** (30 mg, 0.07mmol) and compound **13** (32 mg, 0.07 mmol) were dissolved in a 1/3 mixture of H_2O/MeOH (8 mL). $CuSO_4 \cdot 5H_2O$ (1.8 mg, 0.007 mmol) and Na ascorbate (2.2 mg, 0.014 mmol) were added and the reaction was stirred for 36 h at room temperature. Solvents were evaporated under vacuum, and the crude product was purified via silica gel flash chromatography (CH_2Cl_2/MeOH 92/8) affording product **5** (25 mg, 0.027 mmol, 39%) as colorless oil.

^{1}H NMR (400 MHz, $CDCl_3$): δ = 7.77 (s, 1H, C*H* triazole), 6.82 (br s, 1H, N*H*), 6.35 (br s, 2H, 2 N*H*), 5.56 (br s, 1H, N*H*), 4.69 (s, 2H, OCH_2C-triazole), 4.55 (t, J = 5.2 Hz, 2H, triazole-N-CH_2), 4.50 (m, 1H, NHCONH-C*H*), 4.32 (m, 1H, C*H*-NHCONH), 3.90 (t, J = 5.2 Hz, 2H,

triazole-N-CH_2-CH_2O), 3.70-3.54 (m, 26H, 13 OCH_2), 3.43 (m, 2H, CH_2NHCO), 3.14 (m, 1H, CH_2SC*H*), 2.90 (dd, *J* = 4.4 Hz, *J* = 12.8 Hz, 1H, CH_aH$_b$SCH), 2.73 (d, *J* = 12.8 Hz, 1H, CH$_a$$H_b$SCH), 2.34-2.20 (m, 8H, 4 CH_2), 1.87 (q, *J* = 7.0 Hz, 2H, CH_2), 1.69-1.62 (m, 4H, 2 CH_2), 1.55-1.27 (m, 14H, 7 CH_2), 0.88 (t, *J* = 6.6 Hz, 3H, CH_3); ^{13}C NMR (100 MHz, $CDCl_3$): δ = 173.34, 172.23, 163.93, 144.5, 128.32, 77.98, 76.40, 70.47, 70.18, 70.09, 69.96, 69.87, 69.62, 69.43, 66.11, 65.18, 64.49, 61.83, 60.21, 55.55, 50.24, 40.52, 39.19, 35.86, 35.05, 31.80,29.68, 29.12, 29.04, 28.86, 28.33, 28.18, 28.10, 25.55, 24.18, 22.63, 19.18, 18.74, 14.08; MALDI-MS [M+1] (*m*/z) calcd for $C_{45}H_{76}N_7O_{10}S$, 906.5; found, 906.0. Anal. calcd for $C_{45}H_{75}N_7O_{10}S$: C, 59.64; H, 8.34; N, 10.82; found: C, 59.59; H, 8.35; N, 10.78.

Synthesis of *N*-(11-(4-(13-(β-D-galactopyranosyl-(1→4)-β-D-glucopyranosyloxy)-2,5,8,11-tetraoxatridecyl)-1*H*-1,2,3-triazol-1-yl)-3,6,9-trioxaundecyl)-5,7-hexadecadiynamide (4b)

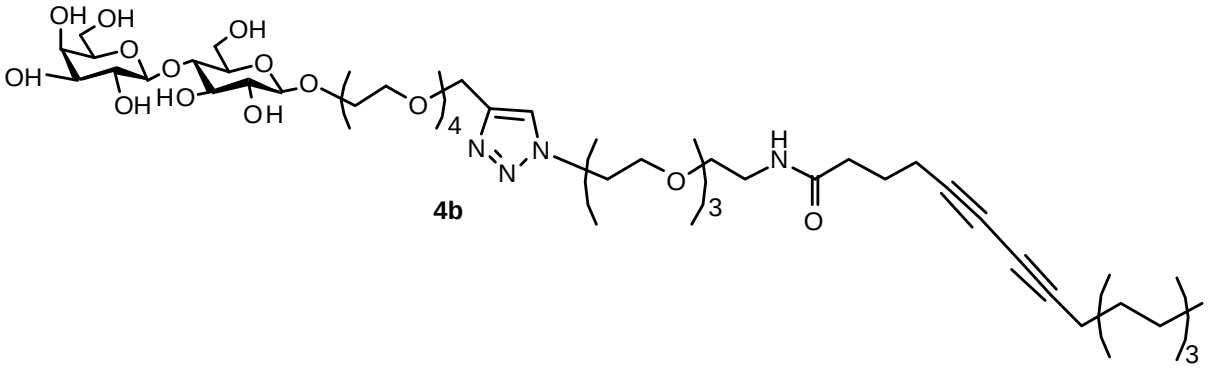

4b

Compound **4a** (55 mg, 0.043 mmol) was dissolved in dry MeOH (12 mL) and a catalytic amount of NaOMe (5 mg) was added to the solution. The reaction mixture was stirred for 2 h, then it was quenched by addition of Amberlite resin until pH≈7 and the solvent was removed under vacuum. The crude product was purified by silica gel flash chromatography ($CHCl_3$/MeOH 6/4), affording product **4b** (20 mg, 0.02 mmol, 46%) as colorless oil. ^{1}H NMR (400 MHz, CD_3OD): δ = 8.06 (s, 1H, C*H* triazole), 4.67 (s, 2H, OCH_2C-triazole), 4.61 (t, *J* = 5.2 Hz, 2H, triazole-N-CH_2), 4.38 (t, *J* = 7.5 Hz, 2H, H-1 and H-1'), 3.95.3.28 (m, 42H, 15 OCH_2 and 12 lactose-H_s), 2.35-2.24 (m, 6H, CH_2-C≡C-C≡C-CH_2 and NHCOCH_2),

1.82 (q, J =7.2 Hz, 2H, $NHCOCH_2CH_2$), 1.53-1.31 (m, 12H, 6 CH_2), 0.92 (t, J = 7.0 Hz, 3H, CH_3); ESI-MS [M+1] (m/z) calcd for $C_{47}H_{81}N_4O_{19}$, 1005.6; found, 1005.4; Anal. calcd for $C_{47}H_{80}N_4O_{19}$: C, 56.16; H, 8.02; N, 5.57; found: C, 56.27; H, 8.00; N, 5.58.

Calculation of the number of anchored HSA molecules

In all reported experiments surfactants and proteins were added into a cuvette containing 1.5 mL of 0.1% v/v bare PnPs dispersion.

Hence, the PnPs net volume in 1.5 mL of dispersion is 1.5 μL = 1.5×10^{18} nm^3.

Given the radius of one PnP (r = 39 nm), the volume of a single PnP is given by $4/3 \times \pi \times (39)^3 = 248348.88$ nm^3.

The number of PnPs in the suspension can be now calculated as

1.5×10^{18} nm^3 / 248348.88 nm^3 ≈ 6.03989×10^{12} PnPs

In the experiment reported in Fig. 6 (in paper text), 43 μL of a 20 μM solution of HSA were added to reach the plateau. Hence:

$(20 \times 10^{-6}$ mol/L) $(43 \times 10^{-6}$ L) = 8.6×10^{-10} mol HSA

$(8.6 \times 10^{-10}$ mol) $(6.022 \times 10^{23}$ $mol^{-1})$ = 5.179×10^{14} HSA molecules

$(5.179 \times 10^{14}$ HSA molecules)/(6.03989×10^{12} PnPs) ≈ 86 HSA molecules/PnP

Calculation of the binding constant

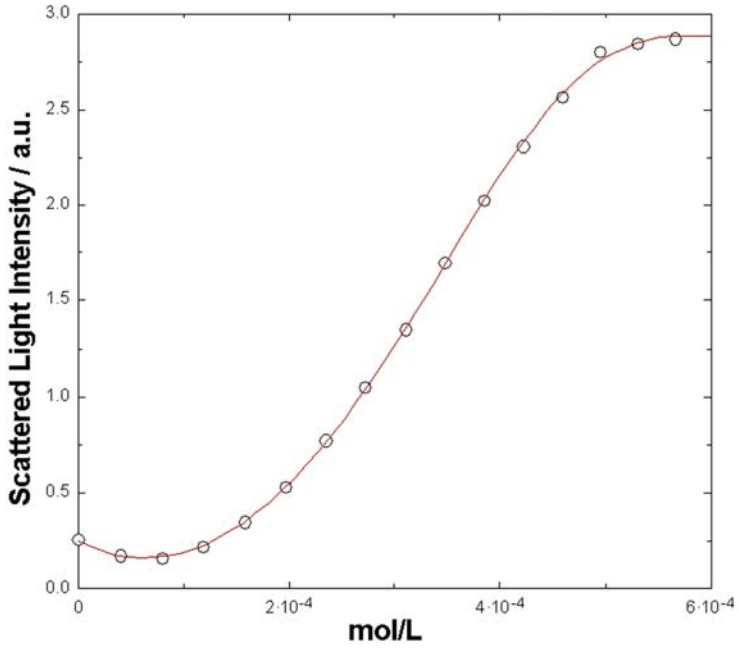

Figure S1. Mean scattered intensity measured for PnPs (open dots) as a function of the concentration of ADM **1** (c_1) present in the dispersion, expressed in molarity (X axis). Line is the best fit obtained from Eq. reported in Ref.[4] Fitting parameters for PnPs: $n_{D\beta M} = 1.4976$, $n_{PnP} = 1.3248$, $n_{H2O} = 1.3319$, $K_d = 6.1 \times 10^{-6}$ M, $r_{NP} = 4.0 \times 10^{-8}$ m.

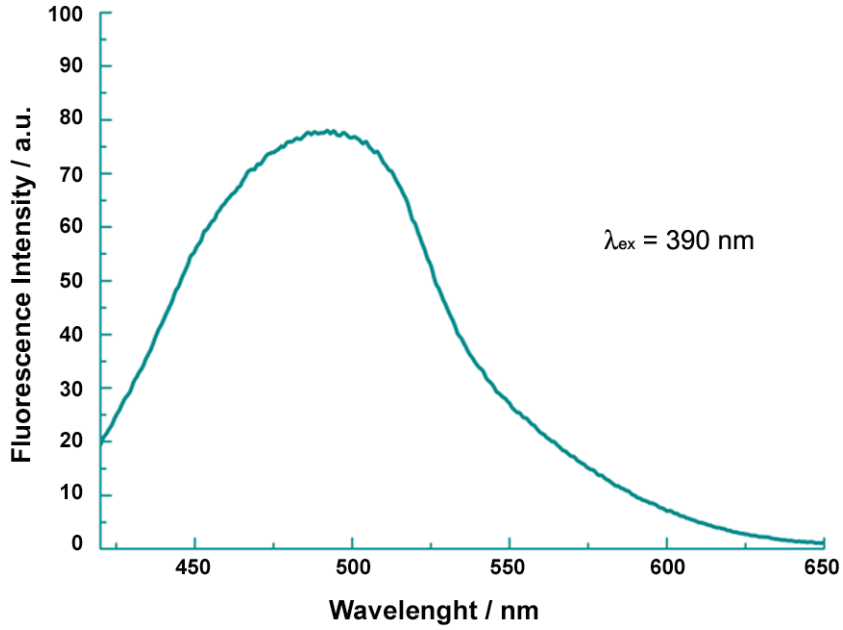

Figure S2. Fluorescence emission scan of a 0.2% v/v water dispersion of PnPs in 10 mM phosphate buffer, pH 7.2, after coating with **1** (5 mM) followed by photopolymerization.

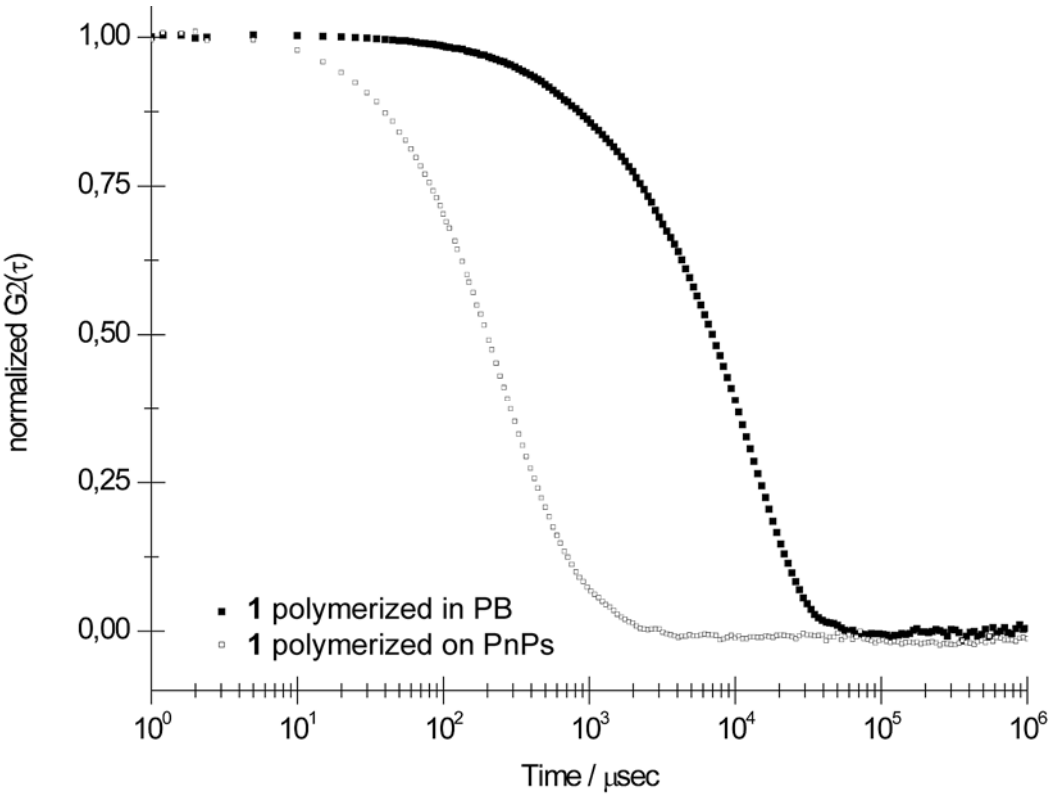

Figure S3. Autocorrelation of the light intensity scattered by **PDA-1** nanoparticles (open squares) and by a micelle dispersion obtained by photopolymerization of a 10 mM solution of ADM **1** in phosphate buffer, pH 7.0 (full squares).

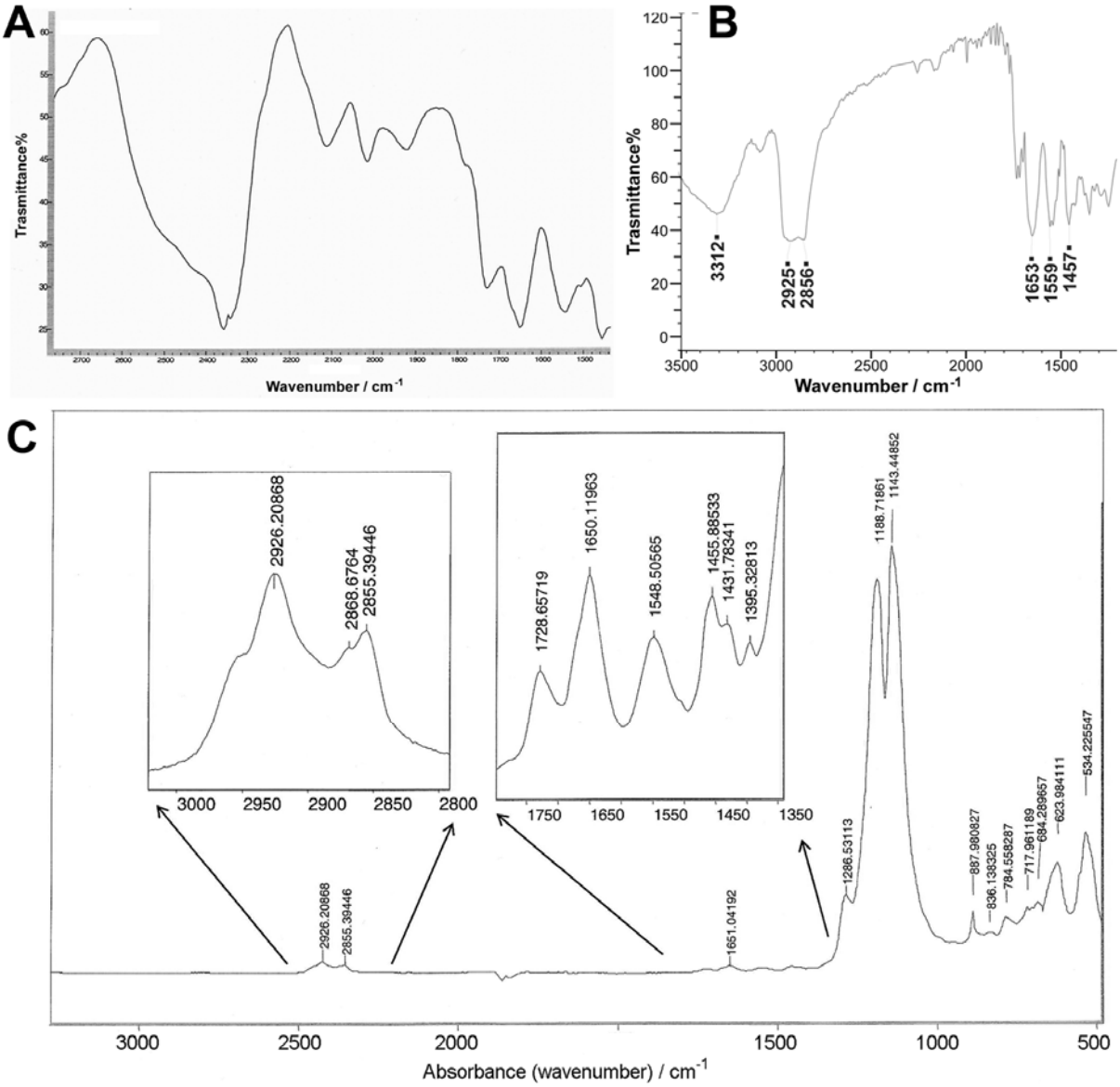

Figure S4. A) Micro-FTIR spectrum of **PDA-1** nanoparticles; B) FTIR of ADM **1**; C) ATR FTIR of **PDA-1** nanoparticles.

References

[1] R. L. Wiseman, S. M. Johnson, M. S. Kelker, T. Foss, I. A. Wilson, J. W. Kelly, *J. Am. Chem. Soc.* **2005**, *127*, 5540.

[2] H. A. Chokhawala, S. Huang, K. Lau, H. Yu, J. Cheng, V. Thon, N. Hurtado-Ziola, J. A. Guerrero, A. Varki, X. Chen, *ACS Chem. Biol.* **2008**, *3*, 567.

[3] F. M. Menger, H. Zhang, *J. Am. Chem. Soc.* **2006**, *128*, 1414.

[4] P. S. Shirude, V. A. Kumar, K. N. Ganesh, *Eur. J. Org. Chem.* **2005**, 5207.

[5] M. Gonçalves, K. Estieu-Gionnet, T. Berthelot, G. Laïn, M. Bayle, X. Canron, N. Betz, A. Bikfalvi, G. Déléris, *Pharm. Res.* **2005**, *22*, 1411.

[6] X.-L. Sun, C. L. Stabler, C. S. Cazalis, E. L. Chaikof, *Bioconjugate Chem.* **2005**, *17*, 52.

[7] S. K. Mamidyala, K.-S. Ko, F. A. Jaipuri, G. Park, N. L. Pohl, *J. Fluorine Chem.* **2006**, *127*, 571.

[8] L. Polito, D. Monti, E. Caneva, E. Delnevo, G. Russo, D. Prosperi, *Chem. Commun.* **2008**, 621.